Sodium in Gramicidin: An Example of a Permion

Ron Elber,* Duan P. Chen,‡ Danuta Rojewska,‡ and Robert Eisenberg‡

*Department of Chemistry, University of Illinois at Chicago, Chicago, Illinois 60680 USA; and *Department of Physical Chemistry, The Fritz Haber Research Center and the Institute of Life Sciences, The Hebrew University of Jerusalem, Givat Ram, Jerusalem 91904 Israel; and ‡ Department of Molecular Biophysics and Physiology, Rush Medical College, Chicago, Illinois 60305 USA

ABSTRACT The reaction path and free energy profile of Na^+ were computed in the interior of the channel protein gramicidin, with the program MOIL. Gramicidin was represented in atomic detail, but surrounding water and lipid molecules were not included. Thus, only short range interactions were investigated. The permeation path of the ion was an irregular spiral, far from a straight line. Permeation cannot be described by motions of a single Na^+ ion. The minimal energy path includes significant motion of water and channel atoms as well as motion of the permeating ion. We think of permeation as motion of a permion, a quasi-particle that includes the many body character of the permeation process, comparable with quasi-particles like holes, phonons, and electrons of solid-state physics. Na^+ is accompanied by a plug of water molecules, and motions of water, Na^+, and the atoms of gramicidin are highly correlated. The permion moves like a linear polymer made of waters and ion linked and moving coherently along a zigzag line, following the reptation mechanism of polymer transport. The effective mass, free energy, and memory kernel (of the integral describing time-dependent friction) of short range interactions were calculated. The effective mass of the permion (properly normalized) is much less than Na^+. Friction varies substantially along the path. The free energy profile has two deep minima and several maxima. In certain regions, the dominant motions along the reaction path are those of the channel protein, not the permeating ion: there, the ion waits while the other atoms move. At these waiting sites, the permion's motion along the reaction path is a displacement of the atoms of gramicidin that prepare the way for the Na^+ ion.

INTRODUCTION

Gramicidin is a small protein that helps ions move through membranes. Roughly speaking, the channel enhances permeation through the membrane in two ways. First, it reduces the energy barrier created by the low dielectric constant of the lipid bilayer (compared with water). Second, the channel tends to maintain (or to provide an alternative to) the solvation shell of the ion. The channel provides interactions (e.g., between carbonyls and the ion) that replace the hydrating waters present in free solution with the solvating carbonyls of its peptide bonds. These short range strong interactions of the ion with water and channel are the focus of the present work.

The most appropriate methods to study these short range forces are calculations with an atomic detail structure of gramicidin. Other methods need to be used when long range forces (e.g., polarization effects across the entire membrane arising chiefly from macroscopic boundary conditions) have important effects on the molecular level, because computation limits the size and duration of simulations in atomic detail. The size of the system is limited to tens of thousands of atoms and the time scale of direct simulation (molecular dynamics) is limited to a few nanoseconds. There is also a conceptual difficulty. The inclusion of short range polarization effects in interatomic potentials, and macroscopic boundary conditions and flux, still poses a significant challenge.

It is therefore important to recognize the restrictions on molecular dynamics (MD) and to focus on the domain in which MD can give meaningful results, i.e., phenomena dominated by short range interactions reasonably independent of macroscopic boundary conditions. Others have made progress in linking short range calculations with long range effects (Åqvist and Warshel, 1989) known to be important in channels (Chen and Eisenberg, 1993a; Chen and Eisenberg, 1993b). However, even the computation of short range effects poses significant problems because of limitations in the duration of the calculations (i.e., in the time scales). Reducing the size of the problem is one way to make these limitations less serious.

The use of a reaction coordinate (Müller, 1980) dramatically reduces the dimensionality of the system (effectively to one dimension) and thus the size of computations. The reaction coordinate is usually defined as the continuous line connecting the reactant and the product in which the energy barrier separating the two states is minimal. The probable path (at finite temperature) followed by an ion (or more precisely the permion) is not necessarily the lowest energy path. Nevertheless, the reaction coordinate provides a useful framework for thermal calculation, because it allows the efficient production of trajectories at sufficiently low energy that they are likely to be near the minimal energy path.

The motion of the permion, the atoms of the protein, water, and permeating ion, as they move along the (multidimensional) reaction path, is much easier to understand than thermal trajectories computed directly by MD. The permion includes only motions relevant to the process under investigation. All other thermal processes are quenched. Atomic

Received for publication 22 August 1994 and in final form 29 November 1994.

Address reprint requests to Dr. Robert S. Eisenberg, Department of Molecular Biophysics, Rush Medical College, 1750 W. Harrison St., Chicago, IL 60612-3824. Tel.: 312-942-6467; Fax: 312-942-8711; E-mail: bob@aix550.phys.rpslmc.edu.

0006-3495/95/03/906/19 $2.00

motions are therefore easier to understand in a calculation of reaction path than in a calculation of a trajectory, which typically includes a considerable number of motions irrelevant to the process of interest, namely permeation.

The permion's path shows chemical interactions hidden by the random motions of typical simulations or by the thermal averaging used in calculations of free energy in these complex (nonequilibrium) systems with coupling reaching from atomic to macroscopic length and distance scales.

The word permion is a new concept and requires definition. It is a quasi-particle in the spirit of solid state physics in which quasi-particles are defined to include some of their interactions with the solid (e.g., electrons in metals), so they better describe the system's dynamics (e.g., phonons in solids). It is important to emphasize that although the experimental observation in channel measurements is of the current carried by an ion entering and leaving the channel, description of the movement of the ion alone does not allow a good representation of the transport process. In fact, the opposite is suggested by the strong coupling observed between atoms of the protein, water, and permeating ion (and their motions) during the permeation process. We shall calculate the properties of the curvilinear coordinate describing the transport process and use it to define a quasi-particle, i.e., a permion.

The permion includes a significant number of atoms, in the same way that a phonon (another particle) describes the coherent oscillations of many atoms in a solid. The permion is completely defined by its effective mass, the effective potential it moves in, and the spectrum of the noise that perturbs its inertial motion along the effective potential. It also has a finite lifetime. The quasi-particle maintains its integrity for long times compared to typical other time scales in the system. A permion lives longer than the vibrational time scale of the channel protein just as a phonon lives longer than a few of its internal oscillations, even when shortened by anharmonicity. Quasi-particles maintain their integrity as long as the internal degrees of freedom of the permion are not too highly excited. For example, the distance between the ion and the nearest waters is essentially the same throughout the reaction path.

The permion consists of the protein channel, the ion, and eight water molecules, as we shall show later. The contribution of different atoms to the reaction path varies very significantly from location to location. That is, at some parts of the reaction path, the ion moves together with the complete water file; in other parts, the atoms of the protein move while the ion and the water file are nearly stationary. The transport process defines the maximal lifetime of the quasi-particle to be in the 100-ns time scale, namely, the time scale of permeation of a single ion, the mean first passage time of stochastic theory (Barcilon et al., 1993; Eisenberg et al., 1995); 100 ns is far longer than the typical period of channel vibrations.

The permion is a useful approximation if two physical conditions are satisfied. One of them is the integrity of the permion. The second is a separation of time scales, as found in many kinetic theories. Specifically, there must be a separation of time scales between the movement of the permion and the rest of the degrees of freedom of the system. We assume that other motions (not included in the permion) are either so fast that they are in thermal equilibrium or are so slow that they are frozen on the time scale of the permion motion. If the other motions are frozen, they can (nearly) be ignored (except for effects on the values and meanings of effective parameters). If the other motions are so fast that they are in thermal equilibrium, the configurations of the rest of the system can be computed either by a MD trajectory of the system or by sampling from the spatial Boltzmann distribution (e.g., by a Monte Carlo procedure). If the system is in fact at equilibrium, both computations should give the same results at a given permion position. In this case, the permion can be described as a (quasi-)particle moving in a system otherwise at equilibrium; the permion is then decoupled from the rest of the system.

If the equilibrium condition is not satisfied, the permion is mixed with other degrees of freedom, and the convenient one-dimensional picture cannot be justified. If the mixing is small, perturbation theory can be used, in the same way that crystal anharmonicity is said to scatter phonons. If mixing is large, the permion is no longer a useful concept. Without time scale arguments, further progress cannot be made.

A simple estimate supports the separation of time scales. Many short range molecular relaxation times that do not include large conformational changes are in the picosecond time scale, much shorter than the hundreds of nanoseconds required for ion permeation. But modes with considerably longer relaxation times may exist that were not detected in the finite time of our simulation, and so this argument is not rigorous. Indeed, the NMR measurements of Cross's lab, which determine the correlation times from NMR measurements of ^2H in gramicidin in a lipid bilayer, North and Cross (1993) and Lee et al. (1993) show that local and global motions occur on a 10–100 ns time scale, the expected time scale of single ion permeation (Barcilon et al., 1993; Eisenberg et al., 1995).

Most of the properties of the permion can be extracted by considering its motion along the reaction coordinate if the assumptions discussed above are sound. For example, the permion potential is the potential of mean force along the reaction coordinate. The friction in the stochastic equation of motion of the permion can be estimated from force fluctuations (noise) along the reaction coordinate via the fluctuation-dissipation theorem (Berne et al., 1990). The effective mass of the permion determines its response to acceleration, its inertial motion. It is determined by a combination of all the masses in the permion and reflects all their properties. Indeed, in solid state physics, the effective mass of a quasi-particle can be negative. In our case, the effective mass is not so mysterious. It can easily be calculated from a Cartesian representation of its coordinate, as shown previously (Verkhivker et al., 1992).

It is essential at this point to clearly identify the separate steps of the calculation that are used to study the properties of the permion. Each step is an independent calculation using

different computational methods to evaluate different quantities. For that reason, the approximations used in one computation do not, in themselves, affect the others. On the other hand, one calculation may use as (one of its) inputs the output of another calculation. Then, the output of the second calculation will depend on another calculation even if they use unrelated formulae and computer programs.

The first step is the calculation of the reaction coordinate itself, namely q, the continuous curvilinear coordinate of low energy that we call the reaction path.

In the second step, we compute the effective potential, the potential of mean force, acting on the permion as it moves along this reaction path. We denote the potential of mean force by $W(q_0)$

$$W(q_0) = -k_B^T \log \int \delta(q - q_0) \exp\left(-\frac{U(R)}{k_B T}\right) dR \quad (1)$$

where R is a vector of all coordinates and $U(R)$ is the full microscopic potential. The Dirac delta function selects a specific value of the reaction coordinate q_0. The integral is evaluated at every value of q_0 of interest.

It is obvious from Eq. 1 that the estimation of the potential of mean force depends on the choice of reaction coordinate; the kernel of the integral is different for different values of the reaction coordinate. The calculation of $W(q)$ uses a previously assumed or computed form of the reaction coordinate.

A reaction coordinate q for ion migration through the gramicidin channel has been computed and reported before (Etchbest and Pullman, 1985). However, previous investigations used less detailed models than that used here. For example, some papers did not include water explicitly. In other studies, the channels were rigid (Pullman and Etchbest, 1977) or a reduced representation of the channel protein was used (Jordan, 1987).

The reaction path was computed in these previous studies by the method of adiabatic mapping. As discussed later and in Materials and Methods, adiabatic mapping is an algorithm likely to produce discontinuous estimates of the reaction coordinate. Such discontinuities defeat one of the main purposes of the calculation; potentials of mean force (and other properties of the permion of interest) estimated along a discontinuous path are likely to be discontinuous as well. Discontinuous estimates of the (actually continuous) potential are not very useful, particularly if the potential needs to be differentiated when used in other calculations, as it nearly always does, because force is the derivative of potential (e.g., the potential of mean force is differentiated in the Langevin equation). We are not aware of a single calculation of the potential of mean force in a channel that used the reaction coordinate in the form it is obtained from adiabatic mapping.

As stated above, the calculation of the profile of free energy, that is, the potential of mean force, uses the estimate of the reaction coordinate as an input. To the best of our knowledge, all previous calculations of the potential of mean force used an estimate of reaction coordinate that ran down the center of the channel, assumed to be a straight line, usually identified as the z axis (see references in the review by Roux and Karplus, 1994). Our calculation of the free energy profile is thus an extension of previous investigations, with a curvilinear reaction coordinate calculated from the structure and microscopic interactions of the protein, not assumed to be a straight line. As is clear from the definition of the potential of mean force (Eq. 1), the potential of mean force will be different along different reaction paths. A calculated curvilinear reaction coordinate is likely to give a more realistic estimate of the potential of mean force than an assumed rectilinear coordinate.

We consider here only the short range properties of the permion, although clearly they represent just a fraction of the relevant interactions during the transport process. For example, the permion interacts with the solvent and the membrane at the permion boundaries and we do not include these interactions with macroscopic boundary conditions, although they clearly can be important in determining the flux of ions through channels in experimental situations. The concentration of permeating ions and electrical potential in the baths surrounding the channel are two macroscopic boundary conditions used to control flux through a channel in many experiments. The potential of mean force that we obtained is thus incomplete (as are, indeed, nearly all potentials of mean force obtained from MD simulations of this type of system). Long range forces need to be included in later work. For now, we are quite confident that the short range forces calculated here determine a permion reaction path that is qualitatively correct; we are less confident of the free energy profile of the permion along the path (see Discussion).

A useful definition of the reaction (or the permion) coordinate is the steepest descent path (SDP). It is continuous and the energy barriers along it are the lowest possible. Methods have been developed to calculate the SDP in small molecular systems (Müller, 1980) and they have proven most helpful in understanding atomic interactions in small systems. Most of them require calculations of second derivatives of the potential or related matrices. However helpful and appropriate for small systems, these techniques are not successful for large systems with more than 100 atoms. The inversion of the relevant matrices becomes expensive and even unstable because a large number of low frequency modes (with eigenvalues close to zero) enter the system as it grows to the size of a protein. It is, therefore, essential to design a different approach that provides a continuous minimal energy path and yet is not limited to small molecules. At this point, it should be emphasized that the widely used approach of adiabatic mapping (Müller, 1980), in which a coordinate is assumed and the energy is minimized with respect to other coordinates, is mathematically and formally ill defined. Adiabatic mapping is especially problematic when a large number of degrees of freedom and local energy minima are involved. Many of the torsions in large systems have multiple minima and the paths computed by the adiabatic

method are likely to be discontinuous. Proteins have a very high density of local energy minima (Elber and Karplus, 1987) and so the reference coordinate used by adiabatic mapping is likely to produce discontinuities in the path between alternate minima as illustrated in the simplified two-dimensional model (Fig. 1) we now discuss in detail in response to several requests.

In the model potential surface shown in Fig. 1 of a fictitious two-dimensional channel, alternating minima in energy are found to the right and to the left of the line down the center of the channel, as in the real gramicidin. The adiabatic calculation starts at the bottom of the figure (say), on the (here vertical) z axis. It moves upward (i.e., forward) one step, and then determines the location x_{min} of the minimum of energy, in this figure, along its (here horizontal) x coordinate. (The z coordinate is held fixed in the calculation whereas the energy is minimized with respect to x.) In this way, adiabatic mapping determines a different value of x_{min} for each value of z and so (typically) yields a curvilinear estimate $x_{min} = f(z)$ of the reaction coordinate. The estimate of the reaction coordinate, namely the function $f(z)$ is, however, frequently also discontinuous, as we shall now see.

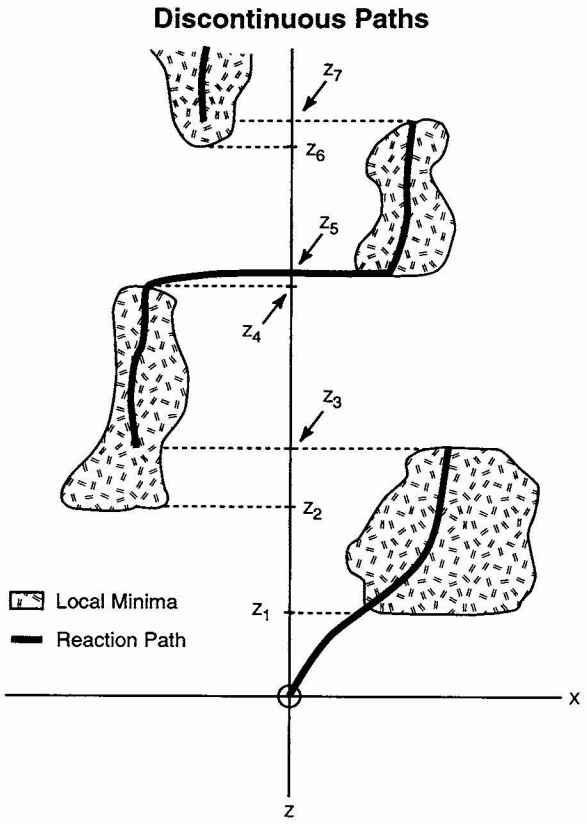

FIGURE 1 Discontinuous estimates of the reaction path. The figure shows the contours of a hypothetical, but not unrealistic, potential surface and the estimate of the reaction path that might arise from adiabatic mapping when alternating minima in energy are present, as they often are in the potential surface of proteins. The minimum on the right extends from z_1 to z_3. The minimum on the left extends from z_2 to z_4. The values of z_j are in ascending order, $z_1 < z_2 < z_3 < z_4$, so the minima on the left and the right overlap in the region $[z_2, z_3]$. An adiabatic calculation (see text) steps along a continuous path as long as that path remains in the concave region of a local minimum. When a further step would take the path out of the concavity of that local minimum, the estimated path tends to jump discontinuously to another concave region, surrounding a different local minimum. Discontinuous estimates of reaction path are not useful because they produce discontinuous estimates of functions, e.g., potentials, that need to be differentiated, a point shown particularly clearly in Fig. 17, as well as in Fig. 7*B* and Fig. 8*B*.

Consider what happens as the adiabatic procedure is used with successively larger values of z. At first, everything is fine; as long as the z coordinate is within the range of attraction of the local minimum (the stippled area in the figure, $z > z_1$; $x > 0$), the adiabatic procedure produces a smooth reasonable estimate. Consider what happens, however, when the path reaches the contour line z_3 that marks the upper edge of the local minimum on the right, where $x > 0$. The minimum on the right extends from z_1 to z_3. The minimum on the left extends from z_2 to z_4. The values of z_j are in ascending order, $z_1 < z_2 < z_3 < z_4$ so the minima on the left and the right overlap in the region z_2, z_3. When z is increased one step more, so $z > z_3$, it moves beyond the region of the local minimum on the right. z moves out of the concave region of the potential surface; the sign of the curvature of the potential surface changes and the potential surface can no longer hold water; z is no longer in the basin of the same local minimum. At this new point $z > z_3$, however, the minimization procedure of adiabatic mapping can still find a minimum in the potential surface, because a minimum still exists for $z > z_2$, but it is a different minimum now on the other side of the x axis. This second minimum is in a different region (of concavity), and the path found by adiabatic mapping has jumped there discontinuously. This example was designed to show the effects of overlapping minima, by making the minima on the right extend from z_1 to z_3 and the minimum on the left extend from z_2 to z_4 with $z_1 < z_2 < z_3 < z_4$. Overlapping local minima like these are present in many proteins and so adiabatic mapping usually yields a discontinuous estimate of the reaction path, as it has in Fig. 1.

In summary, highly flexible proteins have many overlapping local minima, and so adiabatic mapping is likely to produce a discontinuous (estimated) path that cannot be differentiated or used directly in a Langevin equation. In fact, application of adiabatic mapping to a rigid channel (Kim et al., 1985) is probably more sound than application to a flexible channel, because the rigid case has highly reduced dimensionality and fewer minima.

To produce a continuous estimate of the reaction path, and thereby avoid these problems, we use the Self-Penalty Walk (SPW) (Czerminski and Elber, 1990a) technique developed in Elber's lab to compute reaction paths in large molecular systems with multiple local minima. Umbrella sampling (Patey and Valleau, 1973) is then used to calculate the potential of mean force along that estimated path (Verkhivker et al., 1992). The effective mass of the permion and the spectrum of the noise were also calculated.

This manuscript is organized as follows: in the next section we discuss the formulae and the numerical techniques used to calculate the reaction (permion) coordinate; the potential of mean force; the effective mass; and the force-force correlations. The calculations are presented in Results and analyzed there and in Discussion.

MATERIALS AND METHODS

Formulae

The SPW method, described elsewhere (Czerminski and Elber, 1990b; Nowak et al., 1991), provides a continuous path that approximates the SDP. The path is modeled by a hypothetical composite polymer made of many copies of the system, each with the ion at a different location. The energy of the polymer is called S and is given by

$$S = \sum_i V_i + \gamma \sum_i (d_{i,i+1} - \langle d \rangle)^2 + \rho \sum_i \exp\left(- \frac{\lambda d_{i,i+2}^2}{\langle d \rangle^2} \right), \qquad (2)$$

where V_i is the potential energy of a single monomer of the hypothetical polymer. It is also the energy of the system as a whole, the permeating ion, the accompanying waters, and the channel protein itself. d_{ij} is the distance (*rms* in Cartesian space) between monomers i and j, and $\langle d \rangle$ is the mean distance between the monomers averaged over all the monomers. The individual distance between monomers is calculated as follows: let R_i be the coordinate set of the ith copy of the system and R_j be the coordinate set of the jth copy. $\mathbf{R_j}$ is oriented with respect to R_i such that the norm of the vector distance $|\mathbf{R_i} - \mathbf{R_j}|$ is minimal. The minimal norm is called individual distance d_{ij}. The constants γ, ρ and, λ are described in detail elsewhere (Czerminski and Elber, 1990a).

The first term in Eq. 1 includes the sum of the physical energies of the copies of the system. The second term forces all the intermediates to be the same distance apart, thus forcing the intermediates to be equally spaced along the path giving a quite uniform and homogeneous distribution of samples along the reaction path. Intermediates are the copies of the system not in the first or last position along the reaction coordinate, in other words, the copies of the system not including the reactant or product.

The third term is a repulsion term needed to prevent the path from aggregating into a tangle (Czerminski and Elber, 1990a); the lower it is set, the better the approximation to the SDP, provided the path is still continuous. Of course, if the repulsion is too low, the path becomes wildly irregular and folded back on itself, because the trajectory then tends to spend most of its time near the minima. Proper sampling at the barriers is therefore difficult if the repulsion is set to too small a value. As was shown in earlier work (Czerminski and Elber, 1990a), large repulsion (i.e., large ρ or large λ) is equivalent to a system (the permion) moving along the reaction path with high kinetic energy. With very high kinetic energy, the permion in fact follows a straight line path connecting reactant and product, barreling right through a potential energy barrier. With lower repulsion, and thus kinetic energy, the permion cannot penetrate the barrier. Rather, it climbs it. With too low repulsion, and thus kinetic energy, the permion will climb irregularly over the barrier. It will follow a seemingly stochastic path like Brownian motion, doubling back on itself, eventually forming a tangle of trajectories. The value of the repulsion is chosen as low as possible while still giving a monotonic path with a reasonable number of intermediates near the potential barrier, thus providing reasonable sampling of the configuration space of the system near the top of the potential function along the reaction coordinate. The optimized path is found by direct (numerical) minimization of the penalty function defined in Eq. 2 subject to constraints on center of mass translations and rigid body rotations. These constraints eliminate irrelevant degrees of freedom, e.g., those corresponding to the translations of a rigid body. The optimized path is a minimal energy configuration of the hypothetical composite polymer.

The SPW path can be viewed as a particular trajectory of low kinetic energy (Czerminski and Elber, 1990a) mathematically defining (in the present case) the permion. The effective mass of the permion was calculated as described elsewhere (Verkhivker et al., 1992). Let e_i be the slope of the reaction coordinate at the ith position, estimated by

$$\mathbf{e_i} = \frac{R_{i+1} - R_{i-1}}{|R_{i+1} - R_{i-1}|} \qquad (3)$$

where R_j is the coordinate vector of the whole system (protein channel, usually eight water molecules, and an ion) at the jth position along the reaction coordinate. The permion effective mass at the jth position, $M(q_j)$ is the matrix element

$$M(q_j) \equiv \langle e_j | M | e_j \rangle \qquad (4)$$

where M is the effective mass matrix in the Cartesian representation. The effective mass of the permion helps determine its motion along the reaction coordinate according to Newton's laws, written here with the help of the Lagrangian

$$\begin{aligned} L = {} & \tfrac{1}{2}\langle v | e_q \rangle \langle e_q | M | e_q \rangle \langle e_q | v \rangle \\ & + \tfrac{1}{2}\langle v | 1 - e_q \rangle \langle 1 - e_q | M | 1 - e_q \rangle \langle 1 - e_q | v \rangle - U(R) \end{aligned} \qquad (5)$$

Here $|e_q\rangle\langle e_q|$ is a projection operator in the direction of the permion coordinate at the qth position and $(1 - |e_q\rangle\langle e_q|)$ is the complementary projection operator; v is the vector of velocities. The first two terms of Eq. 5 are kinetic energies: the kinetic energy of q and the kinetic energy of everything else. The last term is the potential energy. The projection operator is a function of q and so an alternative notation is possible in which

$$\begin{aligned} \langle v | e_q \rangle = dq/dt; \qquad & \langle e_q | M | e_q \rangle = M(q); \\ \langle v | 1 - e_q \rangle = v'; \qquad & \langle 1 - e_q | M | 1 - e_q \rangle = M' \end{aligned} \qquad (6)$$

M' is the (effective) mass of the rest of the system, the system other than the permion. With this notation, each term in the Lagrangian can be written in two different ways, e.g., the velocity component along q can be written as dq/dt or as $\langle v | e_j \rangle$. In fact, the Lagrangian itself can be written

$$L = \frac{1}{2} M(q) \left(\frac{dq}{dt} \right)^2 + \frac{1}{2} M' v'^2 - U(R) \qquad (7)$$

The momentum along the permion coordinate, namely P_q, is calculated by standard procedure, i.e., $P_q = (\partial L / \partial (dq/dt)) = M(q)(dq/dt)$. It is clear then that the effective mass defined in Eq. 6 above is the conjugate mass for the motion along the reaction coordinate q. We comment that the effective mass M' also depends on q. If averaging is done over the other velocities in the problem, an additional potential term appears in the equations that typically has a weak spatial dependence (Elber, 1990).

One of the long range goals of the work initiated in this paper is to provide a stochastic theory describing the motion of the permion in a reduced way, with a Langevin equation or something like that, simpler and faster to compute than the simulations of MD. The reduced description has advantages that compensate for its lack of atomic detail. For example, it can incorporate boundary conditions and coupling to the macroscopic electric fields. Most importantly, it can directly describe the nonequilibrium systems that are usually used experimentally, in which substantial flux flows and is measured. The reduced description exploits the separation of time scales in channel permeation, by which the motion of the permion is much slower than the motion of its internal degrees of freedom.

To properly reduce the number of degrees of freedom of the problem and to formulate a systematic and rigorous theory, it is important to start from the exact equations of motion for the permion, i.e., by using the usual Newtonian mechanics without applying any reduction. Once the exact equations are written and analyzed in simulations, we have a better chance of deriving the correct reduced equations and parameters for the reduced motion.

The exact equations of motion for the permion can be written by starting with the usual Lagrangian and rotating its coordinate system so that it will be the curvilinear coordinate of the permion as determined in the full (nonreduced) simulations. Eq. 5 is the exact Lagrangian in which one of the coordinates is the permion coordinate. It is evident from the equation that

the effective mass for motion along that coordinate (the permion coordinate) is the mass defined in Eq. 4 and used in the exact Lagrangian (Eq. 5). The effective mass relevant for ion permeation in the real channel will also be averaged over thermal degrees of freedom and will include the effects of external forces and so may differ to some extent from that defined above in Eqs. 4 and 5. Nonetheless, the definitions of Eqs. 4 and 5 are the correct starting place for later work. It is possible that the passage of a permion over a potential barrier in the reaction path will be done in a nondiffusive way, producing flux and other properties different from those of pure diffusive motion. Chiu et al. (1993) report just such properties, having also found highly coherent motion of ion and water during permeation. It is important, therefore, not to assume a diffusive behavior to start with. Rather, one must establish the time scale on which the diffusive model is a decent approximation.

We follow earlier work (Verkhivker et al., 1992) also in the calculation of the potential of mean force and the friction kernel along the discrete representation of the path. Umbrella sampling (Patey and Valleau, 1973) is used in the calculation of the potential of mean force with biasing potential,

$$U_i(R) = k\Delta^2 = k[(R - \mathbf{R}_i) \cdot \mathbf{e}_i]^2, \tag{8}$$

where R is a coordinate set from the trajectory that is used for the sampling and k is the biasing force constant, restricting the trajectory to the neighborhood of the ith position along the reaction coordinate. Δ is the deviation of the trajectory coordinate from the ith position along the reaction path.

We consider next the metric of the reaction path, the variable q. Setting the origin of the reaction coordinate to zero at the reactants, the value of the reaction coordinate q_i at the ith position is defined as

$$q_i = \sum_{j=i}^{i} (R_j - R_{j-1}) \cdot e_j \tag{9}$$

where $R_0 = 0$ (see also Fig. 2). For convenience we shall also use the index of the intermediate structure to denote the location along the reaction coordinate. As the structures along the path are equidistant, q is proportional to the structure index. Note that q defines a single valued function. The position of the ion in the channel, along the z axis, is not necessarily a single valued function and it is in that sense ambiguous. We found such ambiguity (see Results and Fig. 16).

Let $P(q)$ be the thermal probability density of the system to be at q. This function is related to the potential of mean force $W(q)$ by:

$$W(q) = -k_B T \log P(q) \tag{10}$$

where k_B is the Boltzmann constant and T is the absolute temperature. $P(q)$ is related to $P_{U_i}(q)$, the probability density generated in the presence of the biasing potential, by

$$\log P(q) = \log P_{U_i}(q) + \frac{U_i(q)}{k_B T} + C_i \tag{11}$$

where C_i is a constant that is independent of q. Hence, given all the calculated $\log P_{U_i}(q)$, all the $\log P(q)$ can be extracted (up to a global and irrelevant additive constant) by the window matching procedure (Pangali et al., 1979).

Finally, the friction kernel is calculated from the force-force fluctuations. According to linear response theory,

$$\langle \delta F_i(t) \cdot \delta F_i(0) \rangle = 2\pi k_B T \Gamma_i(t), \tag{12}$$

where δF is the random force and $\Gamma(t)$ the memory kernel (Kubo et al., 1991). The $\langle \cdots \rangle$ denotes a thermal average computed here over a trajectory.

We investigated the possibility that the friction may be a function of the position of the permion along the reaction coordinate. The random force at q_i was identified in an empirical way, as the fluctuations of the force along the reaction coordinate for a trajectory at q_i. That is, the coordinate vector R_i was sampled from a thermal distribution at a fixed q_i. With linear constraints, it is easy to generate trajectories at fixed q_i (Elber, 1990). Then,

$$\delta F_i = -\frac{dV_i}{d\mathbf{R}} \cdot \mathbf{e}_i + \frac{dW_i}{dq}, \tag{13}$$

where W_i is the potential of mean force at q_i. Thus, the random force along the permion coordinate is defined as the difference between the mean force and a projection of the full microscopic force sampled from a thermal distribution along q (Straub et al., 1990). It should be noted that the above expression is approximate and leaves out some possible effects (Straub et al., 1990). For example, we do not allow the reaction coordinate to move in response to the presence of the random force.

The thermodynamic average $\langle \cdots \rangle$ in Eq. 12 is calculated by a time average obtained from the trajectory:

$$\langle \delta F_i(t) \delta F_i(0) \rangle = \frac{1}{N_\tau} \sum_{\tau} \delta F_i(t + \tau) \delta F_i(\tau), \tag{14}$$

where N_τ is the number of sampling points we have for a time interval τ. For example, a raw trajectory of 1000 points provides 500 points for the average with an interval $t = 2$ between them. It provides only one point for the average if the interval t is 1000; the statistics (and the accuracy) decreases with increases in the length of the time interval considered.

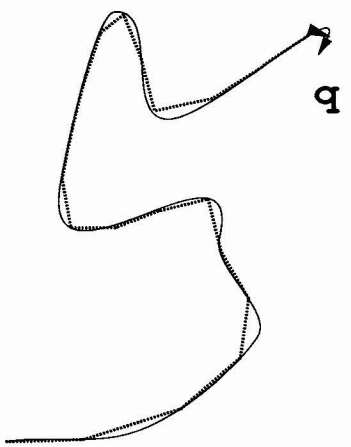

FIGURE 2 The reaction path q (dark line) and segments along it (dotted line). The vertices of the dotted line are the locations q_i of the text.

Computational protocol

The potential energy parameters for the atomic interactions V_i were those of the MOIL program (Elber et al., 1993), a combination of OPLS (Jorgensen and Tirado-Rives, 1988), AMBER (Weiner et al., 1984), and CHARMM (Brooks et al., 1983) force fields. The OPLS determines all the nonbonded parameters, excluding that of the ion; the latter are taken from the literature (Mackay et al., 1984). The AMBER force field is used for almost all the covalent energy terms. Only the parameters for improper energy terms are taken from CHARMM. The water model was TIP3P (Jorgensen et al., 1983). The scaling parameters for the 1–4 interactions were 8 and 2 for the van der Waals and the electrostatic terms, respectively. The dielectric constant was 1 and no cutoff for van der Waals and electrostatic interactions was used.

The reaction path calculations used a discretized version of the action described in the Materials and Methods. The atomic coordinates of the gramicidin ion channel were kindly provided by B. Roux (Roux and Karplus, 1991; Roux and Karplus, 1994). Initial and final structures for the ion transport (reactant and product, the fixed monomers on the edges of the polymer) were computed as follows: the channel's pore was oriented along the z axis and the ion (sodium) was placed inside the channel, with four water molecules flanking it on either side (Fig. 3). The structure was equilibrated and then minimized for 2000 steps with a conjugate gradient routine. The local energy of the reactant and product found by this procedure turns out to be quite large (see below). In the initial structure (the minimized configuration we call the reactant), the ion is already quite deep into the channel, only 6 Å away from the channel center.

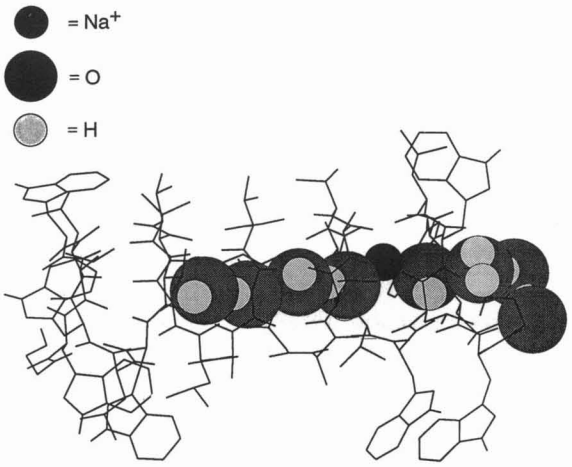

FIGURE 3 The structure of the reactant. The protein channel (gramicidin), eight water molecules, and the sodium ion are at the path starting point.

In this paper, we do not consider the process of ion entry and focus instead on the permion properties inside the channel. We deliberately did not place the reactant position of the permion closer to the end of the channel because the file of waters would then extend significantly into the bath. The 8 or 12 water molecules used in our calculation are unlikely to provide a decent approximation to the bath, or to its dielectric effects. Such calculations will be done in the future. We were also concerned that our approximate boundary conditions do not supply suitable solvation at the edges of the channel. We addressed this issue (in the present context) by repeating the calculation of the reaction path with 12 water molecules instead of 8. The small changes in the properties of the reaction coordinate (see Fig. 9 below) support our conjecture that the permion coordinate (but not necessarily the energy or free energy) is determined primarily by the short range local interactions well described in our model.

Since the channel is symmetric, the structure of the 'products' was obtained by rotating the structure by 180° and renaming the protein residues and the water molecules such that the *rms* deviation of the rotated structure from the original coordinates is minimal.

The SPW algorithm requires an initial guess for the path, that is, a discrete set of coordinates along a path connecting the two end points. We use a straight line (Cartesian) interpolation between the reactant and the product as an initial guess, because it is the simplest and the least biased. The straight line is clearly the trajectory followed by the system in the limit of high kinetic energy, already used in the past as a reaction coordinate for gramicidin (Roux and Karplus, 1991). The final path (the output of the algorithm) is determined by a nonlinear optimization procedure starting from this initial guess.

The very fact that the optimization routine finds a lower energy as it bends the straight line initial guess into a curvilinear reaction path shows the need for the calculation. The two calculations do not yield identical energies; the energy along a curvilinear path is lower than along a rectilinear path. Calculations along a rectilinear path do not reproduce calculations along a curvilinear path, even if the position of atoms along the rectilinear path are chosen to minimize the energy at that location because the minimized coordinate is defined by an adiabatic mapping procedure that, as we have argued previously (in the Introduction), is likely to produce a discontinuous estimate of the path. The two calculations do not yield the same estimate of energy; they do not yield the same coordinates of the atoms of the protein, water, or ion (either relative or absolute); and they do not lead to the same estimates of free energy or other derived quantities.

A nonlinear optimization of the dimension performed here is large. It has 204,417 degrees of freedom which is 3 × (the number of particles = 339) × (the number of grid points = 201). Optimization of such a large system is likely to yield more than one solution. Starting from the above initial guess, the path calculations were repeated four times, varying the number of grid points. For computational convenience (i.e., having a structure exactly at the path center), the code requires an odd number of intermediate points. We used 51, 101, 201, and 401 grid points. The parameters for the path were γ = 2000 kcal/mol Å^2, ρ = 2000 kcal/mol, and λ = 2. The path was optimized for 10,000 steps of the conjugate gradient method of Powell, resulting in a gradient of S smaller than 0.01 kcal/mol Å. The gradient is normalized for one degree of freedom.

To calculate the potential of mean force, the umbrella sampling protocol, described in Materials and Methods, was used. The force constant k was 0.6 kcal/mol Å^2. We tried also k = 1 kcal/mol Å^2 and k = 0.3 kcal/mol Å^2 with similar results. The system was equilibrated for 5 ps and then run (and sampled) for 45 ps, generating the 101 distributions (that we call $P_{U_i}(q_i)$) for the different grid points q_i.

After the equilibration period, overlapping windows were calculated for the most detailed path (the path with 201 points). However, in contrast to the calculation of the minimal energy path, the calculation of the potential of mean force extended only to the middle of the reaction coordinate (to reduce both the machine and human labor involved in this lengthy calculation). By symmetry the second half must be the same. It is important that the calculation of the path of minimal energy (i.e., the reaction coordinate) not be confused with the calculation of free energy. In the calculation of the path we did not assume the symmetry but rather checked for it in the results of the calculations. In particular, we evaluated reliability of the calculation of the (estimate of the minimal energy) reaction coordinate by looking for the symmetry that should be there.

The force fluctuations were computed from a 50-ps trajectory at three fixed positions of q. The projection of the force along the reaction coordinate was saved at each step (of the 50-ps trajectory), providing a sampling of 50,000 points for the calculation of the correlation function (Eq. 8). The force-force correlations were calculated at the start of the reaction coordinate, in the minimal free energy point, and on the barrier in the center of the channel.

RESULTS

Minimal energy path

In Fig. 4 we show three SPW minimal energy profiles: *A-C* are minimal energy paths calculated with 51, 101, and 201 points, respectively. The energy shown includes only the physical forces within the monomers, within each copy of the system. The energy of the repulsion term of Eq. 2 was not included, nor was the energy of the constraining forces that keep the samples equidistant on the reaction path. Although the paths did not converge to the same function, they do have common features. All the paths have a barrier in the middle of the channel approximately 10 kcal/mol high (measured from the lowest energy minimum).

The position of the deepest minimum inside the channel is approximately the same in the three paths of Fig. 4. The two symmetric pairs of barriers (in addition to the barrier in the center) include one pair of barriers closer to the reactant (the starting position of the permion in our calculation) and another pair closer to the center. These barriers are present in all paths. Nevertheless, the paths differ; the greater the resolution of the path, the more atomic details are revealed. Clearly, the calculations have not converged to a unique estimate of the detailed structure of the minimal energy paths. We shall, therefore, restrict the investigation of path properties only to features that are common to all three paths.

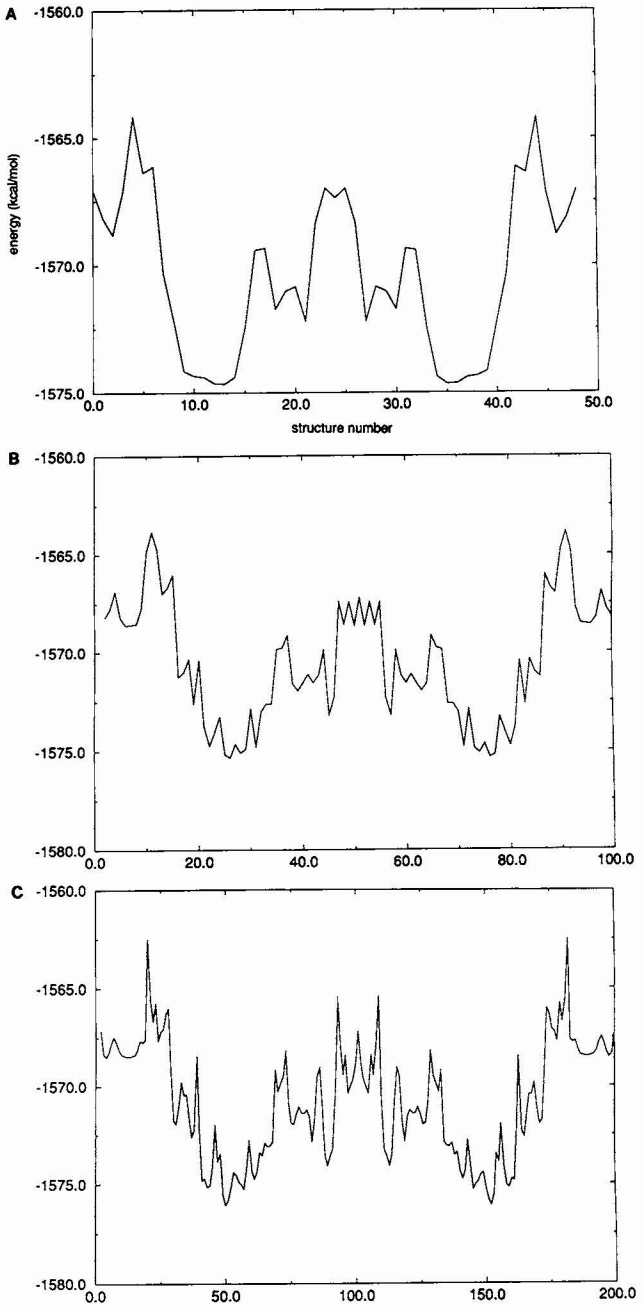

FIGURE 4 Minimal energy paths calculated by the SPW method for ion transport through the gramicidin channel. The paths are shown as a function of the structure number. The only difference between the calculations is the number of grid points. (*A*) A path with 51 grid points; (*B*) a path with 101 points, and (*C*) a path with 201 grid points. Path (*C*) was used for further analysis of the reaction coordinate and in the free energy calculations. See text for more details.

In Fig. 5 we show the atomic structure of the barrier in the middle of the path overlapped with the protein configuration at the beginning of the path. The differences between the two protein structures are not localized. Rather, they spread throughout the protein, suggesting that protein motions that contribute to the reduction in the barrier heights are modes with extended (spatial) low frequency modes. The *rms* deviation between all the α-carbons of the amino acids of the two structures is 0.4 Å.

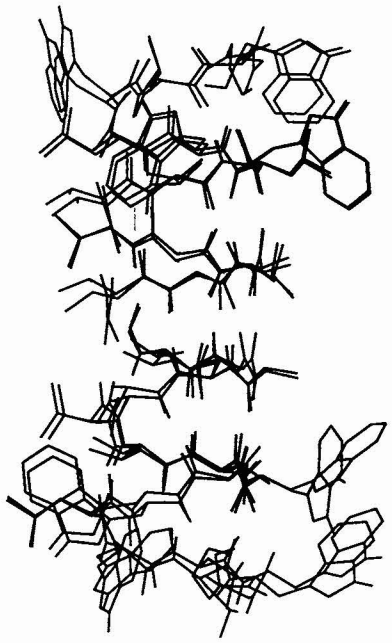

FIGURE 5 The protein structure at the barrier (ion in the channel center). The structure is overlapped with the starting, i.e., reactant configuration.

Complexities of motion

In the simplest possible picture of ion permeation, the reaction path includes only the coordinate of the ion (Roux and Karplus, 1991) and is a straight line. Fig. 6 shows that the path we calculate is not a straight line. We shall soon see that it contains much more than the motion of one ion.

Fig. 6 shows the calculated path of the ion and the protein channel. For simplicity, only a single protein structure (the reactant, namely the starting structure) is shown, and the eight water molecules that were included in the calculations are not shown. It is clear that the ion path is not a straight line. Indeed, the path is not even a monotonic function of the rectilinear coordinate z; it moves nearly at right angles to z in some locations. Waiting sites, in which the ion waits for other particles' motions, are seen along the ion pathway, as we shall soon document.

In a more refined picture of permeation, the whole water file moves coherently with the ion, simply because the ion cannot pass a water molecule in the channel, as has been discussed for many years (and reviewed in Roux and Karplus, 1994). In Fig. 7*A*, we show the z displacement (i.e., displacement perpendicular to the plane of the membrane) of the water molecule in the first solvation shell and the z displacement of the ion. They are clearly highly correlated. Significant (albeit weaker) correlation exists also between the motion of the ion and the motion of the fourth water molecule (Fig. 7*B*). This result supports the previously reported highly correlated motion of the whole file (Chiu et al., 1989; Chiu et al., 1993; and see earlier references in Roux and Karplus,

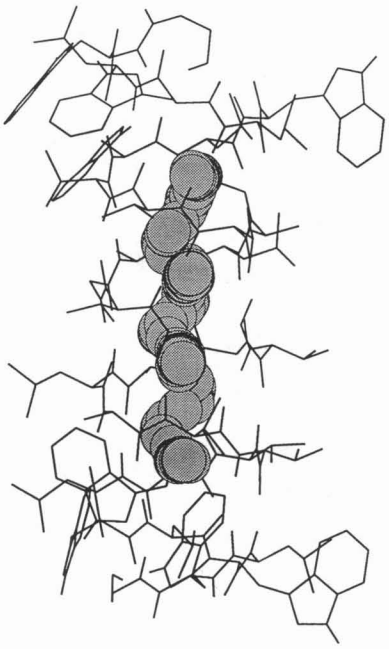

FIGURE 6 The paths followed by the sodium atom through the channel. For clarity only a single protein structure is shown. Furthermore, none of the water molecules is included in the plot. Both flexible protein and eight waters were used in the calculations. Note that the ion motion strongly deviates from a straight line.

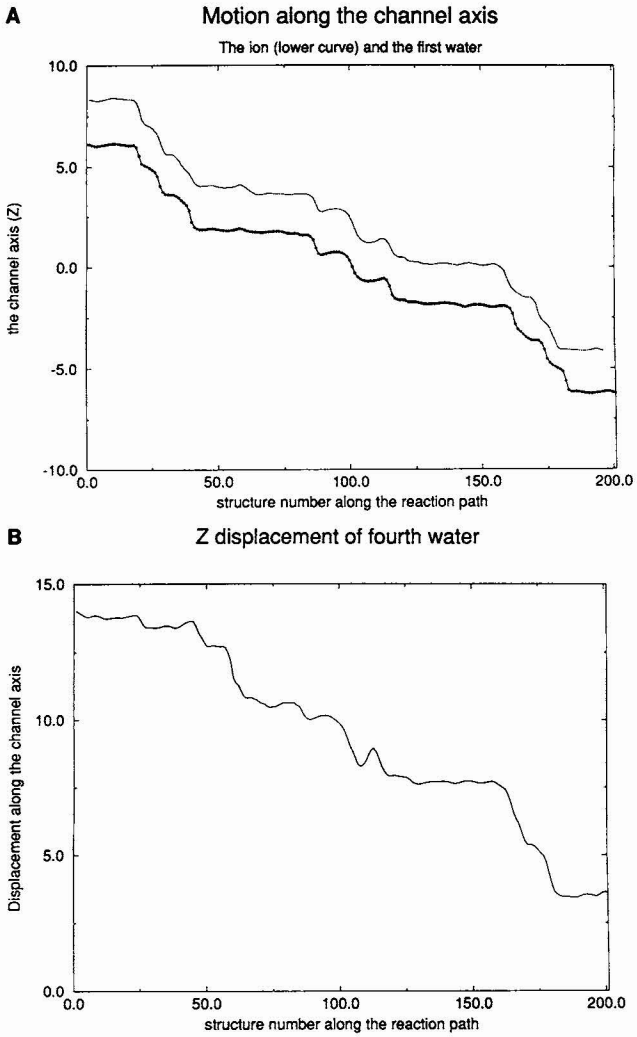

FIGURE 7 (*A*) The displacement of the ion and the nearest water along the *z* axis (perpendicular to the plane of the membrane) as a function of the reaction coordinate (the number of the structure). The displacement is in angstroms. (*B*) The displacement of the ion and the water molecule at the edge of the file. Note that the motion of the water is still correlated well with that of the ion, except near the beginning of the reaction coordinate, where this water molecule is actually outside the channel (see also Fig. 3).

1994). However, the minimal energy path we calculate is more complex than previously reported, perhaps because our model of gramicidin is less subject to ad hoc constraints than those used in earlier calculations of reaction path.

Our results suggest that in addition to the coherent motion of the ion and the waters, it is necessary to include the motions of the channel protein. One way of showing this is to re-examine the *z* coordinate of the ion as a function of the reaction path. In Fig. 7*A* we show that if the permion is moved monotonically along the channel, there are places along the reaction coordinate in which the ion waits; the value of its *z* coordinate hardly changes whereas the value of other coordinates are changing (see also Fig. 8*B*). The visual metaphor used here assumes the permion is dragged through its conformations at a constant rate in time.

In addition to motion along the *z* axis, the ion follows a complex trajectory in the *xy* plane. In Fig. 8*A*, we show the projection of the reaction path on the *x* and *y* coordinate of the ion. The ion rests for a while on the channel walls at positions of maximal coordination (to the water and to the carbonyl oxygens). The plot of the *x* and *y* position along the reaction coordinate shows sharp transitions from one localization site to the next (Fig. 8*B*). As the intermediate structures along the path are equally spaced (in the reaction coordinate, but not in the *z* coordinate), other parts of the system must move while the ion rests. This motion cannot be of the water, because the ion and the water motion is quite coherent (see Fig. 7 for water *z* coordinate) and the ion does not move. In fact, the extra motion is found in the atoms of the channel protein. It is clear then that consideration of the motion of only the ion, or even of the ion and the water, neglects important motions. This is especially true at the waiting sites, the binding sites of state theories of permeation (as reviewed in Hille, 1992).

We were concerned with the effects of the boundary conditions of our calculation on the qualitative properties observed in the simulations. We therefore repeated the calculations with 12 water molecules and 51 grid points. Fig. 9*A* shows the motion of the ion in the *xy* plane and Fig. 9*B* shows the *z* position of the ion as a function of the reaction coordinate. The results are evidently quite similar to those obtained with 8 water molecules shown in Fig. 7*A* and 8*A*.

Clearly, more needs to be done to describe the effects of the entry step, of dehydration and re-solvation on the permeation process. Despite the limitations of our calculations, particularly with regard to the entry step, they are different

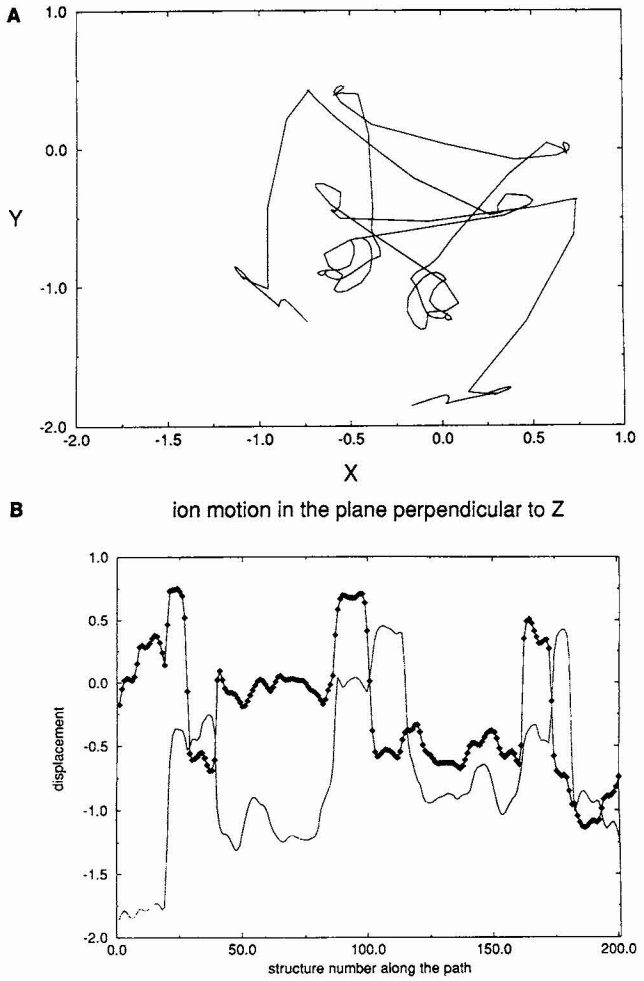

FIGURE 8 Complex ionic motions, with a file of eight waters. (*A*) The ion motion projected to the *xy* plane, the plane perpendicular to the channel axis. The displacement is in angstroms. Note the highly irregular motion of the ion in the plane that accompanies a monotonic motion along the channel axis (Fig. 6*A*). (*B*) The ion motion in the plane perpendicular to the *z* axis. Motion along the *x* axis is shown as a solid line decorated with diamonds and along the *y* axis as a dashed-dotted line; both are plotted as a function of the structure number (reaction coordinate). The displacement is in angstroms.

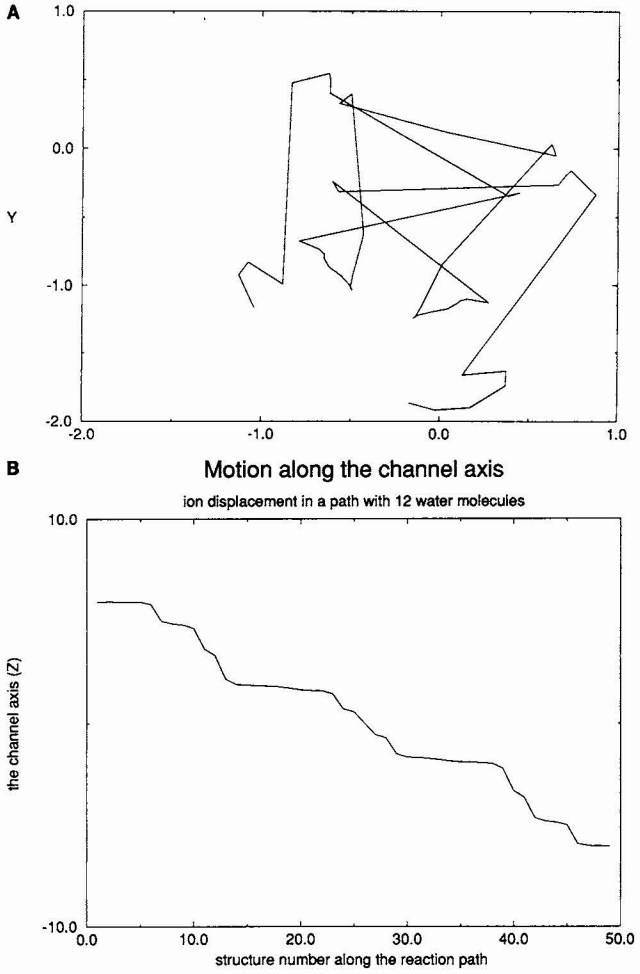

FIGURE 9 Complex ionic motions of a file of 12 waters. (*A*) A computation with a file of 12 waters directly comparable with the computation with a file of 8 waters shown in Fig. 8*A*. The ion motion projected to the *xy* plane, the plane perpendicular to the channel axis. The displacement is in angstroms. Note the highly irregular motion of the ion in the plane that accompanies a monotonic motion along the channel axis (Fig. 6*A*). (*B*) A computation with a file of 12 waters directly comparable with the computation with a file of 8 waters shown in Fig. 7*A*. The displacement of the ion and the nearest water along the *z* axis (perpendicular to the plane of the membrane) as a function of the reaction coordinate (the number of the structure). The displacement is in angstroms.

and complementary to previous calculations made with periodic boundary conditions that severely restrict the dynamics of the protein.

The complexity of motion of the permion can be further seen in the properties of the vectors e_i. These vectors describe the slope of the path at different values of q_i, different positions along the reaction coordinate. The components of $\mathbf{e}_i$, which we call e_{ij}, are the Cartesian elements of the atomic displacements as the structure number moves from q_i to q_{i+1}. If most of the atoms were at rest and only the ion moved between structures i and $i + 1$, then the Cartesian displacements of the ion e_{ij} would be finite (nonzero) but all other values of e_{ij} would be zero. In Fig. 10 we show e_{ij} (specifically, the norm of the atomic components of $\mathbf{e}_i$) as a function of the atom number (i.e., the index used to identify each atom in the structure of gramicidin).

We consider the path slope (i.e., norm of the displacement of all atoms as the structure number changes from q_i to q_{i+1}) at three different positions q_i: (*A*) at the beginning of the path, (*B*) at the free energy minimum, and (*C*) at the barrier in the center of the protein channel. Note that the atom number of the sodium atom is 315 and the atom numbers of the water molecules are 316–339. It is clear from Fig. 10*A* that a very significant number of atoms contribute to the reaction coordinate, at least at this position at the beginning of the path. The motion of the ion or the waters does not dominate. Indeed, most of the water molecules are at rest. Most of the motion is in the protein. The motions within the protein at this reactant site are initial displacements that prepare the way for the permion migration. For example, the displacement of an atom (index number 156) at the COOH terminus

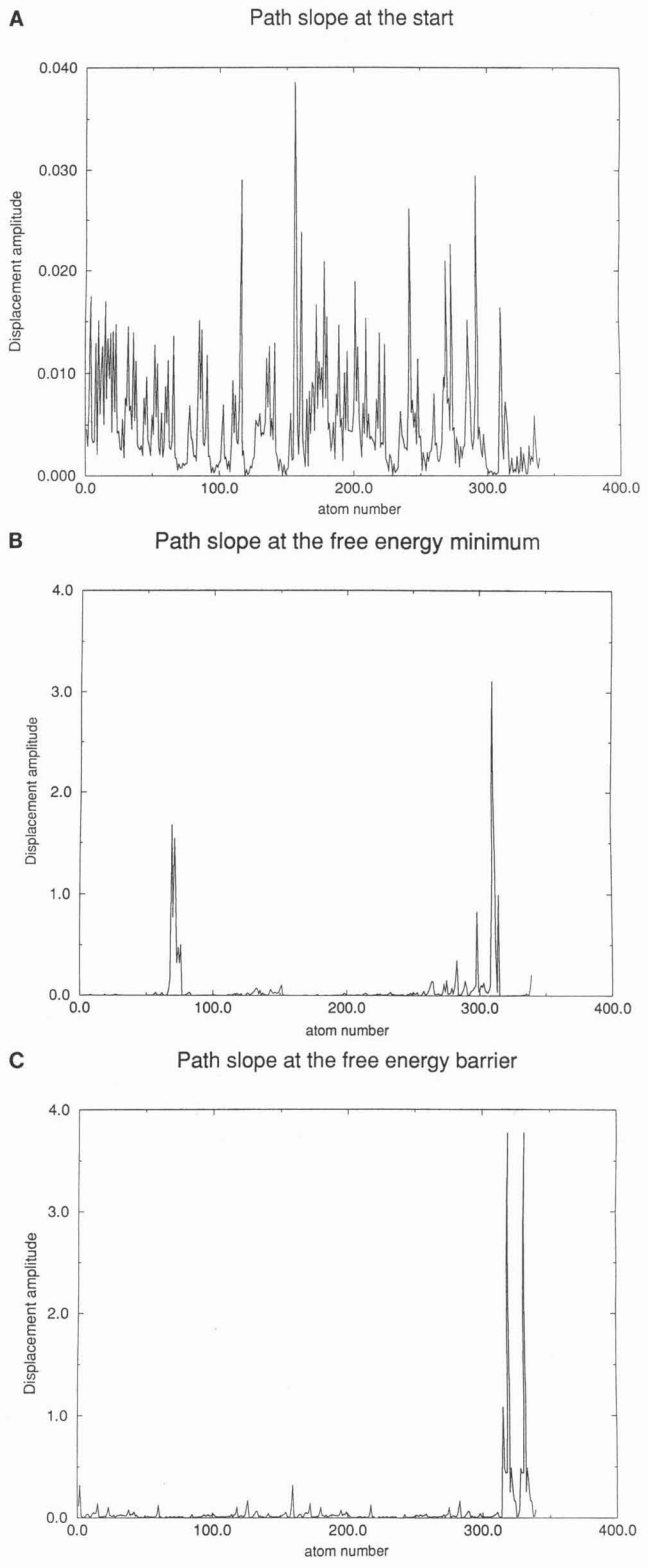

FIGURE 10 The norm of the atomic components of e_{ij}. $\mathbf{e}_i$ is the path slope at the ith position along the path, i.e., e_i is the norm of the displacement of the jth atom as the structure number changes from q_i to q_{i+1}. (A) The components of the first structure (that defines what we mean by reactant); (B) The components at the free energy minimum along the path; and (C) The components at the (central) free energy barrier.

of gramicidin is guiding the motion of the water molecule in the channel. This atom (number 156) is the highest peak in Fig. 10*A*.

It is interesting to contrast the components of motion at this initial site with the motion when the permion is at a different location, namely at the free energy minimum (see Fig. 10*B*). There, the largest displacement within the permion is of a hydrogen atom of a water molecule. There, the water molecule simply rotates (around one of the O-H bonds), thus preserving the position of one oxygen and one hydrogen atom, while displacing the second hydrogen to form a new hydrogen bond with a carbonyl oxygen. The displaced hydrogen of the water is the largest peak in Fig. 10*B*, and the carbonyl oxygen is the second largest peak.

The motions we observe are really quite complex and far from linear (Fig. 6). Furthermore, the motion is never the motion of just the ion. At the reactant position (i.e., the start in Fig. 10*A*) and at the free energy minimum (Fig. 10*B*), significant protein movements are observed. Only at the central barrier is the movement along the reaction path dominated by the ion and the water file (Fig. 10*C*).

Previous investigations of reaction path and dynamics of permeation

The reaction path for ion permeation through the gramicidin ion channel has been investigated many times in the past (Fornili et al., 1984; Kim et al., 1985; Pullman, 1987; Jordan, 1987; Jordan, 1990; Chiu et al., 1989; Chiu et al., 1993). Nevertheless, motions on the level of complexity suggested here have not been observed, either because the models were simplified or the channel protein was restrained. Our calculation, despite its admitted (and evident) limitations is more realistic than many earlier calculations. For example, we did not use a reduced representation of the channel protein (e.g., as a periodic gramicidin with only alanine side chains) or periodic boundary conditions. Correlated motions of the atoms of the protein are probably larger in unrestrained channels. These motions are seen more clearly in the reaction path than in individual trajectories, because trajectories are not computed for long enough durations to observe significant displacement of the atoms. They are seen more clearly in the reaction path than in the potential of mean force because that is thermally averaged and so some atomic details are lost.

The correlations we observe when an ion follows a curvilinear (lowest energy continuous) reaction path suggest a clear mechanistic picture of transport. Indeed, that is why paths are so widely used to help understand the mechanism of chemical reactions; they provide chemical insights hard to develop from stochastic simulations or smoothed estimates of potential of mean force.

Determinants of the energy barriers

It is worthwhile to try to partition the energy along the reaction path into its different components to see how much of

the permeation energy is determined by the channel protein itself and how much is determined by the protein plus water and ion. Fig. 11 shows the energy profile of the reaction path excluding the interactions of the sodium atom. Fig. 12 shows the interactions within the protein only, excluding both the ion and the water. Interestingly enough, the shape of the energy profile (that is, the location of the minima and the barriers) for the waters only path (Fig. 11) is similar to that of the path with ion present, although, of course, the absolute values of the energy and the height of the barriers are modified by the absence of the ion. This is not surprising, because many of the stabilizing interactions with water are lost when the ion is removed. It seems that the essential features of the path are not determined by interactions with the ion but by other forces, say, those between the atoms of the protein and between the atoms of the protein and the water of the channel. Comparisons with the permions of other species of ions, H_3O^+, OH^-, K^+, Li^+, Rb^+, Cs^+, and Tl^+, would be particularly interesting and might reveal much about the mechanism of selectivity in channels (at zero flow, of course), a subject of speculation for more than a century because of its great biological importance (Hille, 1992).

We also calculated the internal energy of just the channel protein excluding both ion and water(s) along the path (Fig. 12). The very different shape of the internal energy profile in this calculation indicates that the protein itself does not determine the positions of the critical barriers for permeation. To be sure, the protein makes a significant contribution to the energy profile (most notably when the water molecules enter or exit the channel at the path edges), but the barriers found in the intact permion are not found in the protein calculated without water or ion. The location of barriers and the permeation properties of the system are properties of the permion, not just the channel protein. It is the location of the whole file—both the waters and the ion—that determines the position of the minima and the barriers along the permion

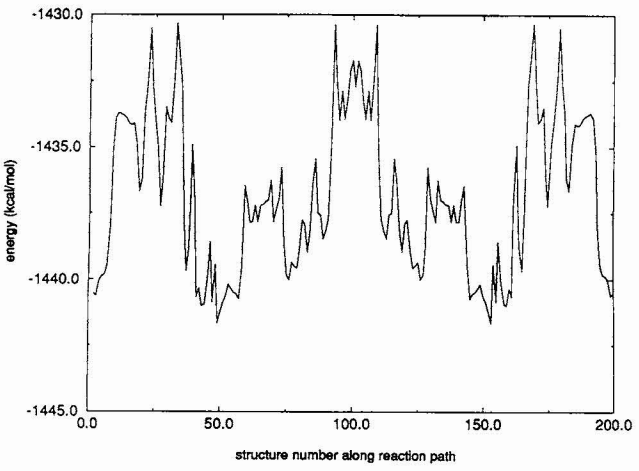

FIGURE 11 The energy along the minimal energy path excluding the interactions of the sodium. That is, the van der Waals parameters and the charge of the sodium were set to zero and the energy of the path was recalculated by using the coordinates of the previously determined SPW path.

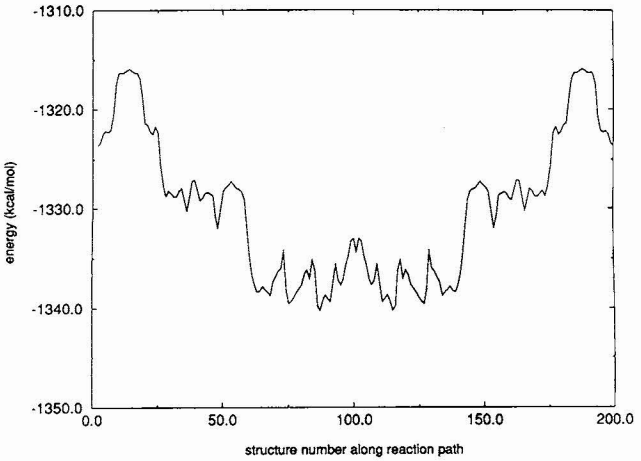

FIGURE 12 The energy along the minimal energy path excluding both the interactions of the sodium and the interactions of the water. Hence, only the internal energy of the protein along the path is plotted.

coordinate. The energy profile of the protein cannot itself determine even the location of the relevant barriers or waiting sites. The energy profile of the protein plus water (without ion) contains, however, the relevant barriers and waiting states. Note that the channel is completely stuffed in our model of 8 waters only when the ion is halfway across the channel. With 12 waters, it is stuffed all the way, which is why we did that calculation, to be sure that the number of waters did not change our qualitative conclusions.

Motion of the permion

The single file movement of the ion and accompanying waters deserves further consideration. Fig. 13 shows the translocation of the ion. Ideally, the ion is solvated by four carbonyls of the channel protein and two nearest waters. For the ion to move, it must lose part of this solvation shell; the carbonyls are fixed in place and cannot migrate with the ion as the waters do. In Fig. 13, *A* and *B*, we show a typical translocation. The ion maintains two of the original four carbonyls while leaning forward towards the two new carbonyls.

The ion motion is of considerable interest, but, as we argued above, it is the motion of the whole file, the permion, if one includes the protein motions, that determines the shape of the energy profile.

How does the permion, the water file plus protein, move? Pictorially, one may think of the file of ion and waters as a polymer, with bonds, angles, and torsions. The bonds are defined as the distances between the oxygen of nearby waters or between the ion and the nearest water molecules. The file may, therefore, move through the channel gliding as a rigid body that preserves its internal structure. Alternatively, the file may use some internal relaxation of (internal) bonds or torsions to help it move through the channel; the permion may worm its way across the membrane. It may employ the stretching and squeezing of bonds, or even the bending of angles like the flapping of the (relatively rigid) wings of a bird.

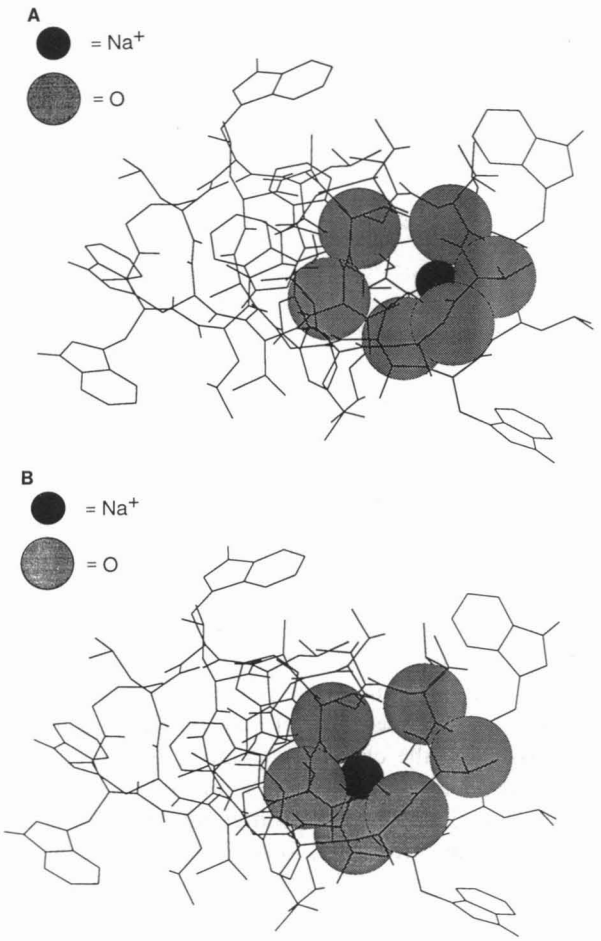

FIGURE 13 Ion translocation. The sodium ion (the dark small sphere) remains hydrated by four carbonyls (large stippled spheres) even as it replaces two hydrating carbonyls (*A*) with two others.

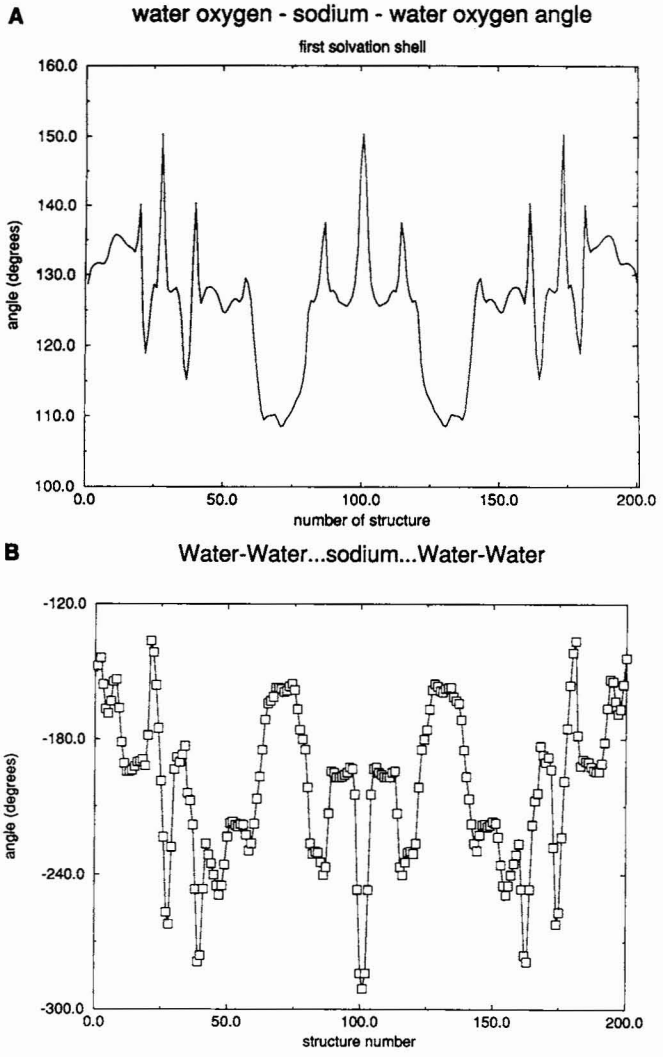

FIGURE 14 Internal degrees of freedom of the permion as a function of the reaction coordinate. (*A*) The angle between the sodium and the oxygen atoms of the nearest waters; (*B*) The torsion defined by the two nearest waters and the two waters next nearest to the ions.

In Fig. 14 we show two of the internal coordinates of the file, namely the nearest and the next nearest waters to the ion, as a function of the reaction coordinate. In Fig. 14*A* we show the angle between the sodium and the nearest waters' oxygens. In Fig. 14*B* we show the torsion defined by the four oxygens of the nearest and the next nearest waters. The changes of the angle are not small (they are 40°); however, they do not correlate with the minimal energy profile. Only at the central barrier does this angle flatten allowing the permion to glide. Another interesting feature are the large changes (the spikes of 120°) in the torsion in Fig. 14*B*. These correlate well with the position of the energy barriers in Fig. 4*C*, suggesting that the permion is a flexible file, a polymer with internal torsional excitation, resembling a worm wiggling its way through the channel. It is not a rigid plug (made of waters and an ion) that pushes through the channel. The permion moves like a linear polymer made of waters and ion, following the reptation mechanism of polymer transport (de-Gennes, 1971). Ions and water move coherently along a zigzag path dominated by local interactions with neighbors, constrained in their wiggles by the channel protein.

Permion effective mass

In Fig. 15 we show the effective mass of the permion as a function of position (i.e., of the structure number). Note that our definition of the effective mass (and the metric of the coordinate) implies that the effective mass of the permion is a weighted average of the masses of all the atoms that contribute to this quasi-particle. The variation in the permion effective mass is self-evident and is maximal at the position of the maximum of the free energy profile. Two points are worth emphasizing. First, the permion effective mass is never even close to that of the sodium (23 amu) or potassium ion (39 amu). They are in fact both below 11.7 amu, which is less than the mass of the carbon. Second, the changes in the effective mass are not small; the changes are ~5 amu. So, whatever the permion is, and it is definitely not a sodium or potassium atom, its effective mass changes significantly with position.

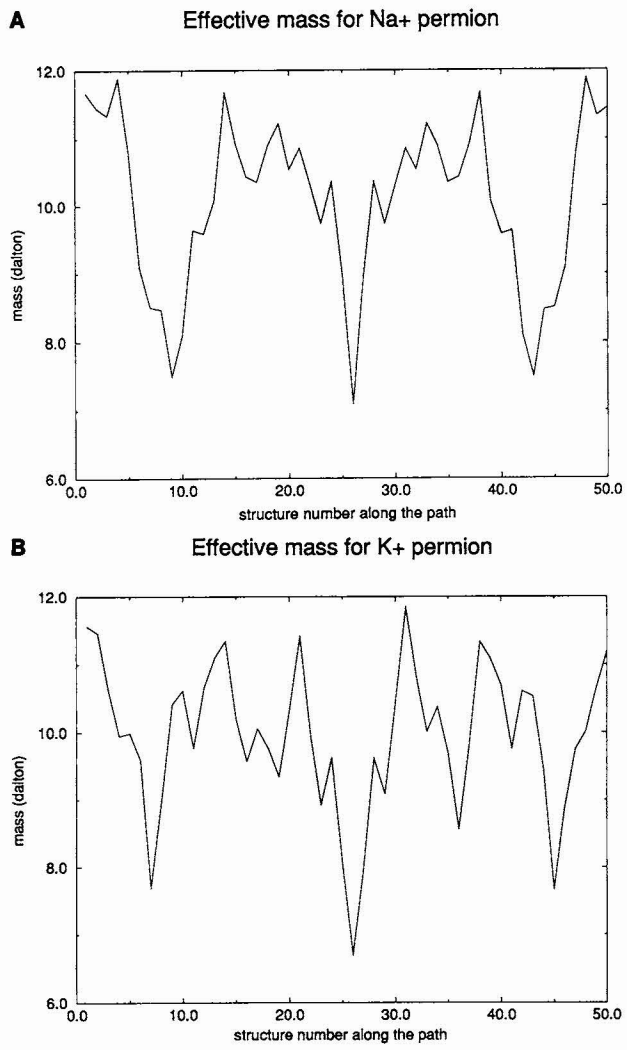

FIGURE 15 The permion effective mass as a function of the reaction coordinate. (*A*) A permion formed around a Na^+ ion; (*B*) A permion formed around a K^+ ion. See text for more details.

Free energy profile

The free energy profile is shown in Fig. 16. Note that the abcissa only shows the 100 structures actually calculated. The other symmetrical part of the free energy profile is not shown. It is reassuring that the size of the barrier in the channel is similar to that found in experiments (Andersen and Koeppe II, 1992). In our present calculation, the free energy profile has a significant barrier at the center of the channel. There are three barriers around structures 10, 30, and 45. Deep minima are at structure 40 and at structure 77.

The free energy profile was the most difficult of all the permion properties to calculate. It is also the result with the largest error bars. There are two sources of estimation errors. The first source is statistical and human, namely, errors in doing the window matching. We estimate this error to be approximately 1 kcal/mol, uniform throughout the reaction path. The second source of errors is systematic and is

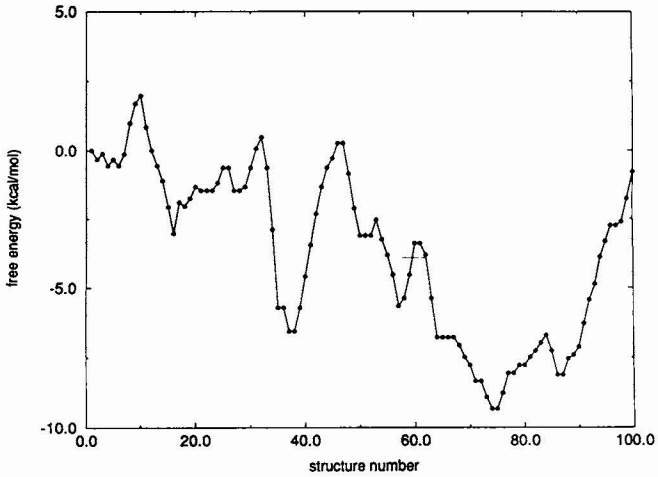

FIGURE 16 The free energy profile calculated along the curvilinear reaction (i.e., minimal energy) path, shown as a function of location along that path. The free energy was calculated at 101 intermediate points, reaching only to the center of the (symmetric) path. The graph shows only the points calculated and so extends halfway through the channel, unlike the other graphs in this paper.

harder to estimate. As discussed in the Introduction, our calculation did not include long range forces or the effects of boundary conditions in the bath that determine potential and concentration there. Such effects need to be included in simulations if they are to predict actual (nonequilibrium) experimental results, and we shall try to include them in the future, along with the short range forces calculated here.

Our present calculations lead to the following expectations of qualitative properties of a complete calculation. It is expected that the closer the ion is to the channel mouth, the stronger is the dielectric screening provided by the long range solvent forces. Hence, the present free energy profile will sit on a broad potential with a central barrier that monotonically decreases towards the channel edges (when the transmembrane potential is zero) (see references to the substantial literature on this subject in, for example, Roux and Karplus, 1994). This is consistent with the calculations previously reported (Åqvist and Warshel, 1989). The magnitude of the corrections due to the long range forces is not clear and it is likely that these will depend on experimental conditions. We finally comment that other permion properties calculated in this section are expected to be significantly more accurate than the free energy profile.

The rectilinear reaction coordinate

We must comment here on the common representation in the literature of the channel as a profile of free energy along the z axis, i.e., along an assumed rectilinear coordinate. In the absence of a better estimate of the reaction coordinate, such graphs have a role. But once a reaction coordinate is calculated and shown to be highly curved and not even single valued in z, the assumption of a straight line coordinate is difficult to defend.

Fig. 17 shows what happens if free energy is plotted as a function of z. The free energy is hard to understand in such a plot because it is a multiple valued function of the straight line coordinate. A multiple valued function cannot be differentiated or then used in equations involving spatial derivatives, such as in a Langevin or Fokker-Planck equation. A multiple valued representation of free energy is inappropriate and quite inferior to a single valued representation (Figure 16).

Other properties of the permion

To complete the description of the permion as a one-dimensional particle moving stochastically along the reaction path, we need to calculate one more function, the friction or the memory function that describes the response of the rest of the system to the motion along the reaction path. Simple stochastic models assume that the memory is very short, giving an effective friction constant in time (see Discussion). In more sophisticated models the friction is assumed to be a function of time and the time dependence gives rise to an integral over time history.

Interestingly, we find that the friction varies substantially with location. It is a strong function of location as well as time. We are not aware of previous investigations in channels in which the memory function was found to depend strongly on position, although strong dependence has been seen in another biomolecule (Verkhivker et al., 1992).

Fig. 18 shows the force-force correlation function (that is proportional to the memory function (Berne et al., 1990)), at different locations. In Fig. 18*A* the memory function at the reactant (i.e., the starting position) is plotted. The friction at the reactant position decays rapidly from a high initial value of 90 to much less than 10 in 1 ps, indeed nearly in 0.1 ps. There are very fast oscillations (but with small amplitude) superimposed on a slower oscillation with a period of 0.5 ps.

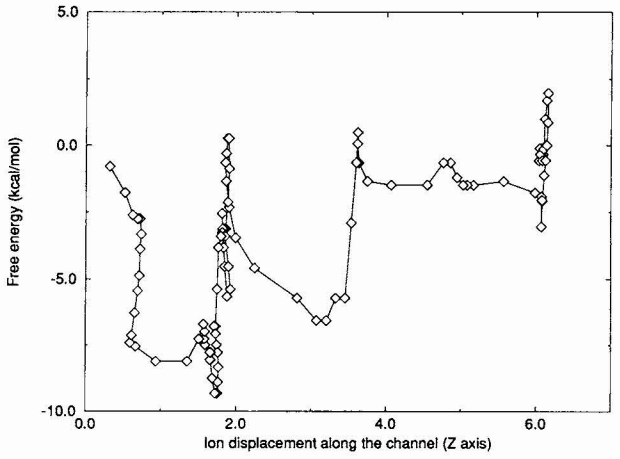

FIGURE 17 The free energy profile shown as a function of the rectilinear coordinate z, not the reaction coordinate. The free energy is hard to understand in such a plot because it is a multivalued function of the straight line coordinate. Such a multivalued function cannot be differentiated or used in derivative calculations, such as in a Langevin or Fokker-Planck equation.

The major decay takes place in the first 100 fs. Although all 50,000 points (sampling an interval of 50 ps) were used to calculate the force-force correlation time, each point of duration 1×10^{-15} s, the correlation time is less than 1×10^{-12} s, 1 ps, 2% of the interval.

The friction is strikingly different at the free energy minimum (Fig. 18*B*) and at the top of the free energy barrier (Fig. 18*C*). On the top of the barrier (Fig. 18*C*), fast decay of the memory function is evident, which primarily reflects the motion of the file of waters. Fig. 18*D* shows the two memory functions (at the free energy minimum and maximum) at a shorter time scale of just 100 fs. The force-force correlation function on the top of the barrier has a smaller initial value. It further oscillates between positive and negative values even after 10 fs, suggesting that the integral (from $t = 0$ to $t = \infty$) over the correlation function (that finally yields an estimate for the total friction) will be smaller at the barrier than at the free energy minimum. The integral over the memory function (which we call Γ) provides an estimate of the static friction to be used in a suitably reduced Langevin equation. Hence, on the barrier it seems that the permion feels considerably less friction than at the minimal free energy position.

The effect of the reduced friction on the rate of permeation is unfortunately hard to predict. It will tend to enhance the rate because the diffusion constant $D = k_B T/m\Gamma$ for crossing the barrier is larger. However, it will also tend to slow down the rate because recrossing is more likely to occur. A complete calculation of stochastic permeation is necessary (Eisenberg et al., 1995) to evaluate the overall effect.

To summarize, we obtain a complex behavior for the memory function, similar to the complex behavior of the slope of the reaction coordinate that varies significantly along the path.

DISCUSSION

This section is divided into two main parts: the first, the more philosophical, explains our view of ion transport in models with atomic detail and the second addresses a number of physical results obtained from the present calculations.

Significant progress has been made in understanding the microscopic structure of the gramicidin channel. However, connecting the structural information to properties of ion transport, i.e., experimental measurements of current, still poses a significant challenge to theory. Straightforward calculations in atomic detail are restricted to times (1 ns) that are too short to describe transport across the channel (160 ns per ion per picoamp of current). Methods that do not include straightforward integration of equations of motion (e.g., transition state theory and reduced stochastic equations; more details are provided below) are approximate. Care must be used when translating the microscopic properties of atomic detail models to the stochastic or statistical parameters of the approximate models. The translation to statistical parameters is usually associated with time scale arguments, and a priori assessment of time scale separations is difficult.

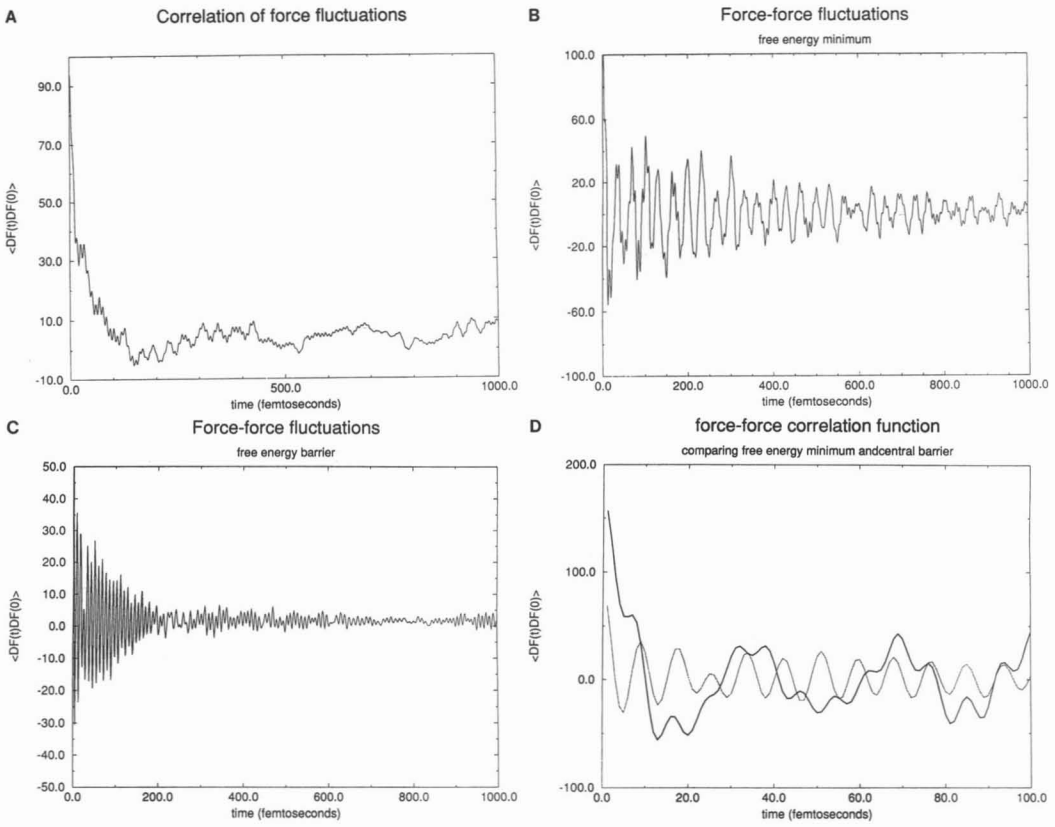

FIGURE 18 Force-force correlation function at particular positions along the reaction coordinate. (*A*) At the starting position where we call the permion the reactant; (*B*) At the free energy minimum; (*C*) At the free energy barrier. (*D*) Comparison of the correlation function at the free energy minimum and at the free energy barrier for the period of 100 fs only.

For example, in transition state theory, which has been used to describe ion transport, there are two main assumptions. First, a dividing surface of no return separates the reactant and product part of the potential energy. That is, if the molecule crosses the dividing surface once, it never returns. Second, the motion in the direction perpendicular to the dividing surface is assumed to be much slower than the motion within the dividing surface. A substantial separation of time scales is assumed.

It is possible to correct for the no return assumption of the transition state theory if the flux through the system (including any number of recrossings) is calculated and compared with the flux of transition state theory, the ratio being called the transmission coefficient. It is not clear, however, that the transmission coefficient can be calculated (except in a formal way) without solving the entire flux problem (the problem of the full Langevin equation, with boundary conditions and potential barriers of any shape (as in Eisenberg et al., 1995).

Just as significant is the second point, the assumed separation of time scales, even though it is sometimes ignored. If the time scale of motion in the dividing surface is not different from the time scale of crossing it, the calculation of the transmission coefficient becomes as difficult as a calculation of MD in atomic detail. In this case, the whole concept of a transition state is not useful. Ignoring the second point may lead to the misconception that the transition state theory can be made exact (in a useful and general way) by calculating the transmission coefficient or solving a one-dimensional projection of the full flux problem.

Similar discussion applies to the construction of stochastic equations from microscopic models (e.g., the generalized Langevin equation). Choice of irrelevant coordinates to be integrated out is not arbitrary. The irrelevant coordinates must approach equilibrium faster than the slower ones; otherwise, they are relevant.

It is therefore crucial, when a statistical or stochastic model is proposed, to choose as carefully as possible the relevant and irrelevant coordinates, satisfying the requirement of separation of time scales. Although a rigorous approach or solution to the above problem is not known, at least to us, one must still address the problem and provide the curvilinear reaction coordinate, that of the permion, not the ion, appropriate for subsequent calculations (e.g., using the Langevin equation).

In this manuscript, we attempt to address this problem. We try to identify relevant and irrelevant coordinates for ion permeation. We base our analysis on the following observations or assumptions. First, at temperatures that are not too high, molecular systems tend to follow the minimal energy paths. Therefore, we pick the minimal energy path as the most likely coordinate to be followed by the permion. Sec-

ond, motions on the length scale of a few angstroms or less are considerably faster than large scale motions (of tens of angstroms or more). It is therefore possible that some of the slower time relaxation processes of the lipid membrane or of the solvent will occur on time scales comparable with ion transport. Approximations that are based on time scale separation are not necessarily appropriate for the simultaneous treatment of short range and long range coordinates. Alternatives, e.g., continuum theories, are necessary when long scale phenomena are present because long range forces (arising for example from macroscopic boundary conditions determining in part the local potential gradient) can be important at all time scales. Pure time scale arguments are not necessarily applicable; spatial scales must also be considered.

We therefore break the problem of permeation into two parts and consider in this manuscript only the short range interactions (under equilibrium conditions, i.e., no transmembrane potential) for which time separation is more likely to occur. This leads us to the permion picture. The coordinate that defines the permion is the lowest energy path that takes into account short range interactions only. The permion is the one-dimensional coordinate that approximately accounts for all short range interactions. It allows a significant reduction in the complexity of the system.

Once the permion picture is established, we can continue to construct our stochastic model, a generalized Langevin equation of the form:

$$\frac{\mathrm{d}}{\mathrm{d}t}\left(M(q)\frac{\mathrm{d}q}{\mathrm{d}t}\right) = -\frac{\mathrm{d}U_{\mathrm{eff}}}{\mathrm{d}q} - \int_0^t \Gamma(t'-t)\frac{\mathrm{d}q(t')}{\mathrm{d}t'}\,dt' + \delta F \tag{15}$$

where U_{eff} includes both the potential of mean force and the long range forces. δF is the random force. $M(q)$ is the effective mass as discussed and defined earlier, e.g., in Eq. 6 in the discussion of the Lagrangian of the system.

The effective mass of a permeating ion has not been considered before (to the best of our knowledge) and so needs further discussion. The effective mass of a quasi-particle may be quite different (or even have a different sign) than that of a closely related real particle. For example, the electron quasi-particle of semiconductor physics has thousands of times the mass of a real electron and (in some situations) can have a negative sign. The reason is, of course, that the effective mass depends on the properties of the entire system, the permion in our case; the effective mass of the Lagrangian (Eq. 6) is the natural and appropriate estimate we use for the effective mass in the generalized Langevin equation but it need not be even approximately equal to the actual mass of the permeating ion.

All the functions in the above equation were computed. However, the model is clearly incomplete because long range forces were not included. The long range forces are likely to change the effective potential and part of them must be solved self-consistently with the permion motion (because both have similar time scales). Nevertheless, we expect the coordinate of the permion that is determined by short range interaction to remain the same even after long range forces are included. The long range forces see the permion as an average and are not likely to change the permion shape (coordinate). This is the reason we focus below on results directly related to the coordinate. The results are significant because the reaction coordinate we extract is quite different from that used in the past.

We also tried to establish a separation of the time scales, at least approximately, by calculating the memory function along the reaction coordinate. As is clear from Fig. 18, the memory function decays rapidly, suggesting that the motion in the plane perpendicular to the permion coordinate is in equilibrium. However, it is important to emphasize that memory functions extend over many many orders of magnitude of time so they can have long tails containing large areas even if they appear to vanish in some plots. Indeed, it is not clear that memory functions must (at all times) be decreasing functions of time, although obviously they must eventually decrease fast enough (asymptotically to zero, at a rate faster than t at long times) to be integrable (over an infinite interval of time) if the generalized Langevin equation is to be useful. So the equilibration in our calculation is uncertain; the memory calculation was done over a finite time, by using the approximations of a frozen coordinate and of linear response theory.

Another interesting result of the present calculations is the cooperativity of the motion of the ion, water, and the channel. Channel permeation is not a process in which a bare ion is transported through a pipe. Rather, a complete water file, coupled to the channel motion, is moved (Figs. 7 and 14) as seen in previous simulations (Chiu et al., 1993). Sequential motion is also evident in our calculation. First, the water file and the ion move and then the file waits for protein movement to reduce the barrier to the next binding site (see Figs. 7 and 9).

A reaction coordinate that includes large contributions of other atoms (besides the permeating ions) may explain why different ions have similar transport properties (Andersen and Koeppe II, 1992) in gramicidin. We described in Results that the ion must be partially desolvated from the carbonyls as it propagates through the channel. The process of carbonyl solvation and de-solvation is expected to depend strongly on ion properties such as size. Smaller size means stronger local solvation and therefore slower transport rate. An inverse trend is expected from size arguments. For example, the radius of K^+ and Na^+ determined from ionic crystals is 1.33 and 0.97 Å, respectively (Lide, 1990). Thus, there is a 30% change in radius and therefore a very large difference in the energy of the first solvation shell. To estimate the electrostatic energy, we set the distance between the carbonyl oxygen and the ion to be σ, the usual van der Waals radius. Using the combination rule of the OPLS force field (Jorgensen and Tirado-Rives, 1988) in which $\sigma_{ij} = \sqrt{(\sigma_i\sigma_j)}$, the energy difference Δ is ~14 kcal/mol, ~24 kT. And transport rates

tend to vary as $\exp(\Delta/kT)$, which here is some $\exp(24) \approx 3.0 \times 10^{10}$, not a small number. The fact that standard chemical models imply such sensitivity of permeation to a 0.36 Å change in diameter came as a surprise, to at least some of us, and seems to raise important questions for traditional theories of selectivity in channels (reviewed in Hille, 1992). Biological selectivity is rarely more than a factor of $10 = \exp 2.3$ and $10 \ll 3 \times 10^{10}$. Biological (equilibrium) selectivity might arise from very small differences in the average location.

The above estimate suggests that very large differences in transport should be observed for different ions, due to the large changes in the interactions with the channel. Nevertheless, the transport properties of different ions are found to be quite similar in experiments on gramicidin (Andersen and Koeppe II, 1992). This result is easy to explain in terms of the movement of a permion. Once the ion properties are averaged with the properties of many more particles (waters and protein atoms) to make the permion quasi-particle, the difference between permions containing different types of ions is much reduced. To further demonstrate this point, we also calculated the reaction coordinate for the K^+ cation. Fig. 15*B* shows the effective mass of the permion for this system, K^+ in gramicidin. The similarity between Na^+ in gramicidin and K^+ in gramicidin is evident (Fig. 15, *A* and *B*, respectively).

It is important to point out that comparing ion transport in water and in a channel can be misleading. In water the ion moves with a solvation shell, forming a quasi-particle that apparently has not yet been given the name it deserves. The size of the quasi-particle depends on the strength of the electric field at the ion's surface. The smaller the ion, the larger the solvation shell in free solution. Thus, different ions look more alike in water than their crystal radii (or energetic calculations based on those radii) would suggest. However, inside the channel the ion is separated from most of the waters that solvate it in free solution. In gramicidin, these are mostly replaced with carbonyls. In other words, the permion has quite different structure from the ion-water complex in free solution. It also has quite different dynamics as the ion moves. The hydrating groups in free solution move along with the ion (for the most part), but inside the channel the solvating carbonyls are (more or less) static and need to be replaced as the ion moves from site to site. Thus, the solvation of the ion in the channel is very different from its solvation in free solution. Ion transport in free solution must be expected to be quite different from ion transport inside protein channels, although based on the same principles, just as it is in polymers (Nitzan and Ratner, 1994). The permion is different from the ion hydration quasi-particle of diffusion in free solution.

To summarize, in this paper we suggest a new view of ion transport. We suggest that the transport is done along coordinates more complex than a straight line path of one ion. We extract properties of this coordinate and name it as a new quasi-particle, a permion. Defining a permion helps contrast the properties of ions in channels with those in water.

We thank Benoit Roux for many useful discussions through the years and for providing us unpublished material. We thank Henry Orland for pointing out the similarity between permion motion and the reptation mechanism. R. Elber is a West Fellow of the University of Illinois and an Alon Fellow at The Hebrew University supported there by a grant from the Israel Science Foundation. The Fritz Haber Research Center is supported by the Minnerva Fund. D. Rojewska was supported by National Institutes of Health training grant to the Departments of Physiology at the Universities of Illinois and Rush. R. Eisenberg and D. P. Chen were supported by grants from the National Science Foundation.

REFERENCES

Andersen, O. S., and R. E. Koeppe II. 1992. Molecular determinants of channel function. *Physiol. Rev.* 72:S89–S158.

Åqvist, J., and A. Warshel. 1989. Energetics of ion permeation through membrane channels, solvation of Na^+ by gramicidin A. *Biophys. J.* 56: 171–182.

Barcilon, V., D. P. Chen, R. S. Eisenberg, and M. A. Ratner. 1993. Barrier crossing with concentration boundary conditions in biological channels and chemical reactions. *J. Chem. Phys.* 98:1193–1212.

Berne, B. J., M. E. Tuckerman, J. E. Straub, and A. L. R. Bug. 1990. Dynamic friction on grid and flexible bonds. *J. Chem. Phys.* 93: 5084–5095.

Brooks, B. R., R. E. Bruccoleri, B. D. Olafson, D. J. States, S. Swaminathan, and M. Karplus. 1983. CHARMM: a program for macromolecular energy minimization and dynamics calculations. *J. Comput. Chem.* 4:187–217.

Chen, D. P., and R. S. Eisenberg. 1993a. Charges, currents, and potentials in ionic channels of one conformation. *Biophys. J.* 64:1405–1421.

Chen, D. P., and R. S. Eisenberg. 1993b. Flux, coupling, and selectivity in ionic channels of one conformation. *Biophys. J.* 65:727–746.

Chiu, S.-W., J. A. Novotny, and E. Jakobsson. 1993. The nature of ion and water barrier crossings in a simulated ion channel. *Biophys. J.* 64:98–109.

Chiu, S.-W., S. Subramaniam, E. Jakobsson, and J. A. McCammon. 1989. Water and polypeptide conformations in the gramicidin channel: a molecular dynamics study. *Biophys. J.* 56:253–261.

Czerminski, R., and R. Elber. 1990a. Self-avoiding walk between two fixed points as a tool to calculate reaction paths in large molecular systems. *Intern. J. Quant. Chem.* 24:167–186.

Czerminski, R., and R. Elber. 1990b. Reaction path study of conformational transitions in flexible systems: applications to peptides. *J. Chem. Phys.* 92:5580–5601.

Eisenberg, R. S., M. M. Klosek, and Z. Schuss. 1995. Diffusion as a chemical reaction: stochastic trajectories between fixed concentrations. *J. Chem. Phys.* In press.

Elber, R. 1990. Calculation of the potential of mean force using molecular dynamics with linear constraints: an application to a conformational transition in a solvated dipeptide. *J. Chem. Phys.* 93:4312–4321.

Elber, R., and M. Karplus. 1987. Multiple conformational states of proteins: a molecular dynamics analysis of myoglobin. *Science.* 235:318–321.

Elber, R., A. Roitberg, C. Simmerling, R. Goldstein, G. Verkhivker, H. Li, and A. Ulitsky. 1993. Moil: a molecular dynamics program with emphasis on conformational searches and reaction path calculations. *In* Statistical Mechanics, Protein Structure and Protein-Substrate Interactions. S. Doniach, editor. Plenum Press, New York. In press. (This program is available via anonymous ftp from Internet sites at addresses 128.248.186.70 or 132.64.96.20.)

Etchbest, C., and A. Pullman. 1985. The gramicidin A channel: comparison of the energy profiles of Na^+, K^+, and Cs^+. *FEBS Lett.* 193: 125–134.

Fornili, S. L., D. P. Vercauteren, M. Welti, and E. Clementi. 1984. Water structure in the gramicidin-A transmembrane channel. *Biochim. Biophys. Acta.* 771:151–164.

Gennes, P. D. 1971. Reptation of a polymer chain in the presence of fixed obstacles. *J. Chem. Phys.* 55:572–579.

Hille, B. 1992. Ionic Channels of Excitable Membranes, 2nd ed. Sinauer Associates, Sunderland, Massachusetts.

Jordan, P. 1987. Microscopic approach to ion transport through transmembrane channels the model system gramicidin. *J. Phys. Chem.* 91:6582–6591.

Jordan, P. 1990. Ion-water and ion-polypeptide correlations in a gramicidin-like channel. *Biophys. J.* 58:1133–1156.

Jorgensen, W. L., J. Chandrasekhar, and J. D. Madura. 1983. Comparison of simple potential functions for simulating liquid water. *J. Chem. Phys.* 79:926–935.

Jorgensen, W. L., and J. Tirado-Rives. 1988. The OPLS potential fields for proteins, energy minimizations for crystals of cyclic peptides and crambin. *J. Am. Chem. Soc.* 110:1666–1671.

Kim, K. S., D. P. Vercauteren, M. Welti, S. Chin, and E. Clementi. 1985. Interaction of K^+ with the solvated gramicidin A transmembrane channel. *Biophys. J.* 47:327–335.

Kubo, R., M. Toda, and N. Hashitsume. 1991. Statistical Physics II, Non-equilibrium Statistical Mechanics, 2nd ed. Wien-New York: Springer-Verlag, Vienna and New York.

Lee, K.-C., H. Wu, and T. A. Cross. 1993. ^2H NMR determination of the global correlation time of the gramicidin channel in a lipid bilayer. *Biophys. J.* 65:1162–1167.

Lide, D. R., ed. 1990. CRC Handbook of Chemistry and Physics, 71st ed. Boston: CRC Press, Boston.

Mackay, D. H. J., P. H. Berens, and K. R. Wilson. 1984. Structure and dynamics of ion transport through gramicidin A. *Biophys. J.* 46:229–248.

Müller, K. 1980. Reaction path on multidimensional energy hypersurfaces. *Angew. Chem. Int. Ed. Engl.* 19:1–13.

Nitzan, A., and M. A. Ratner. 1994. Conduction in polymers: dynamic disorder transport. *J. Phys. Chem.* 98:1765–1775.

North, C. L., and T. A. Cross. 1993. Analysis of polypeptide backbone T_1 relaxation data using an experimentally derived model. *J. Magnetic Resonance* 101B:35–43.

Nowak, W., R. Czerminski, and R. Elber. 1991. Reaction path study of ligand diffusion in protein: application of the self-avoiding walk (SPW) method to calculate reaction coordinates for the motion of Co through leghemoglobin. *J. Am. Chem. Soc.* 113:5627–5637.

Pangali, C., M. Rao, and B. J. Berne. 1979. A Monte Carlo simulation of the hydrophobic interaction. *J. Chem. Phys.* 71:2975–2981.

Patey, G. N., and J. P. Valleau. 1973. The free energy of spheres with dipoles: Monte-Carlo with multistage sampling. *Chem. Phys. Lett.* 21: 297–300.

Pullman, A. 1987. Energy profiles in the gramicidin A channel. *Quart. Rev. Biophys.* 20:173–200.

Pullman, A., and C. Etchbest. 1977. The effect of molecular structure and of water on the energy profiles in the gramicidin A channel. *In* Ion Transport through Membranes. K. Yogi and B. Pullman, eds. Academic Press, New York. 277–293.

Roux, B., and M. Karplus. 1991. Ion transport in a model gramicidin channel: structure and thermodynamics. *Biophys. J.* 59:961–981.

Roux, B., and M. Karplus. 1994. Molecular dynamics simulations of the gramicidin channel. *Annu. Rev. Biophys. Biomol. Struct.* 23:731–761.

Straub, J. E., B. J. Berne, and B. Roux. 1990. Spatial dependence of time-dependent friction for pair diffusion in a simple fluid. *J. Chem. Phys.* 93:6804–6812.

Verkhivker, G., R. Elber, and Q. H. Gibson. 1992. Microscopic modeling of ligand diffusion through the protein leghemoglobin: computer simulations and experiments. *J. Am. Chem. Soc.* 114:7866–7878.

Weiner, S. J., P. A. Kollman, D. A. Case, U. C. Singh, C. Ghio, G. Alagons, S. P. Jr., and P. Weiner. 1984. A new force-field for molecular mechanical simulation of nucleic acids and proteins. *J. Am. Chem. Soc.* 106:765–784.